



Agenzia nazionale per le nuove tecnologie, l'energia e lo sviluppo economico sostenibile

RADON PASSIVE DETECTORS INTERCOMPARISON IN FIELD IN MARIE CURIE'S TUNNEL AT TERME DI LURISIA

RESULTS

Authors:

Francesco Cardellini, Enrico Chiaberto, Luisella Garlati, Federica Leonardi,
Mauro Magnoni, Elena Serena, Rosabianca Trevisi, Miriam Veschetti

Intercomparison's working group:

Luisella Bardi, Francesco Cardellini, Enrico Chiaberto, Luisella Garlati,
Daniele Giuffrida, Federica Leonardi, Mauro Magnoni, Gianfranco Minchillo,
Anna Prandstatter, Ivo Riccardi, Elena Serena, Rosabianca Trevisi,
Rosamaria Tripodi, Miriam Veschetti

Under the patronage of:



In collaboration with:





Agenzia nazionale per le nuove tecnologie, l'energia e lo sviluppo economico sostenibile

Acknowledgements

We would like to thank the owners of the Lurisia Terme for hosting us so kindly during the whole period of the intercomparison's works. A special thank is due in particular to Claudio Magnaldi for the continuous support, allowing us to access to the measurement site in any circumstances.

Many thank also to the Roccaforte di Mondovì Municipality for granting us the use of the "Centro Polivalente" for our Congress. Finally we would like to thank Luca Gentile for having made available his deep knowledge of Lurisia and its fascinating history.

Under the patronage of:



In collaboration with:





Indice

1.	Introduction: health risk, radon measurements and intercomparisons	4
2.	Metrological aspects	6
2.1	<i>The INMRI primary reference radon source in air</i>	6
2.2	<i>The control of the primary system</i>	7
2.3	<i>Effects of the density of the air</i>	7
2.4	<i>The calibration of the monitors used during the Lurisia intercomparison</i>	7
3.	The Lurisia Tunnel: the radiometric characterisation of the site	11
3.1	<i>Radiometric characterisation</i>	11
3.2	<i>Environmental monitoring</i>	16
4.	Logistics and evaluation of the exposures	19
5.	Results and discussion	26
5.1	<i>Presentation of the data</i>	26
5.2	<i>Statistical analysis</i>	40
6.	Conclusions	44

Under the patronage of:



In collaboration with:



1. Introduction: health risk, radon measurements and intercomparisons

Radon is an important health issue since many decades: more than sixty years ago, in 1951 William F. Bale gave for the first time the correct scientific explanation of the health risk due to the radon exposure. In fact, Bale understood for the first time that the radon progeny, deposited in the lung and in particular in the bronchial epithelium, was responsible of the release of a considerable amount of dose. Twenty years later the first epidemiological studies showed a clear relationship between the increased incidence of the lung cancers and the cumulated radon exposures among miners. From that moment, studies on radon spread all over the world. It was very soon clear that, in many cases, very high radon concentrations, much greater than those usually found in the free atmosphere, could be measured not only in mines but also in normal dwellings. During the last decade of the XX century, several epidemiological studies confirmed the carcinogenicity of radon even for the domestic exposures.

All these studies, based on long lasting radon measurements (several months or even years) in thousands of dwellings, need adequate equipment. The necessity of radon detection techniques, able to make measurements in a simple and cheap way, lead the researchers to develop some devices, the dosimeters, based on the passive detection of the α radiation: the devices are placed at the measurement sites for a convenient period and then return to the laboratory for the analysis.

The nuclear physics already had many instruments suitable for radon detection; therefore, in most cases, the issue was to adapt some existing devices developed for other purposes (neutron and cosmic rays measurements, etc.).

In Italy, for example, the first National Radon Campaign (1989-1995) was performed using a dosimeter based on the CR-39 and the LR-115 nuclear tracks etch detectors.

In the following years, the request of a more adequate traceability and accountability of the radon measurements gave rise to many intercomparison exercises. These exercises, organized by institutes such as NRPB (UK) and BfS (Germany) were performed in “radon chambers”, where not only the radon concentration but also all the main environmental parameters (temperatures, pressure, humidity) are strictly controlled.

However, very soon, the growing of “in-field” experiences put on the light that the extremely controlled conditions typical of the “radon chamber” intercomparisons were too distant from the “real condition” encountered in the real houses and workplaces where the dosimeters are usually exposed. For that reason the idea of an “radon in-field intercomparison” began to appear, in spite of the great experimental difficulties, a useful tool to investigate the behaviour of the passive detection systems in real conditions.

A first, very interesting experience of this kind was done in Spain in 2012 [1].

Following the promising results obtained in this first event, we planned a similar exercise in Italy.

Therefore, starting from these ideas and reflections, AIRP, the Italian Radiation Protection Association, with the aid of many other national institutions, such as, ARPA Piemonte (the Environmental Protection Agency of Piemonte), ENEA-INMRI (National Institute of the Metrology of Ionising Radiation), Politecnico di Milano, INAIL (Italian National Workers

Compensation Authority) and FANR (Federal Authority for Nuclear Regulation, United Arab Emirates), organized in 2014 the “radon passive detectors in-field intercomparison” in the Marie Curie’s Tunnel, in Lurisia, a thermal location in the South-West of Piedmont.

The proposal was quite successful: 46 laboratories subscribed, the 20% of which non Italian, and sent us their devices to be exposed in Maria Curie’s Tunnel, that is a very special location. Here the most radioactive water in Europe springs (with a radon concentration greater than 25000 Bq/l) and here, in 1918, Marie Curie came in search of new radium mines.

Nowadays, the Tunnel is still an important place, suitable for testing measurement devices and for radiation protection experiments. The environmental conditions in the Tunnel are quite severe: very high radon concentrations (well above 10000 Bq/m³) and a relative humidity that approaches the 100%. the Tunnel is a special place where radon measurements devices can be tested in very extreme conditions.

The Congress, held in Lurisia the 7th-8th of May 2015, was the final step of the work done with the intercomparison exercise: during these days it was possible not only to discuss together on the intercomparison’s results, but also to share and confront opinions on many other radon issues, such as monitoring campaigns, remedial actions and many other topics.

This report, however, is entirely focused only on the intercomparison results, that is the “core” of this meeting. The “in-field measurement” is a very important and tricky issue: the transfer of the measurements procedures from the laboratory to the open field is not an easy task. If this event and this brief publication will help to clarify some aspects and problems related to this issue, we will have achieved the goal. The judgement to the reader.

2. Metrological aspects

The reference radon concentrations in the Tunnel were measured using six different monitors, made available by ARPA Piemonte, INAIL, JRC ISPRA and Politecnico di Milano: three Alphaguard (AG sn. 933, 1311 e 1312), based on an ionisation chamber and three MR1 (sn. 19, 46 e 50), based on a scintillation cell. All the monitors were calibrated in the INMRI Laboratory, at the ENEA Casaccia Research Centre.

The calibration procedures of the monitors follow basically the steps:

- The efficiency and background (blank) evaluation
- The study of the influence of the environmental parameters
- The quality control procedures

In the next paragraphs we will describe briefly the INMRI primary reference radon source and we will discuss the influence of the environmental parameters on the response of the instruments.

2.1 The INMRI primary reference radon source in air

The INMRI primary reference radon source in air is showed in Figure 2.1. It is used to calibrate all the reference monitors of the INMRI. It consists of an aluminium flask whose volume is 111.77 liters, one radon monitor (a scintillation cell) and a group of radon sources. All the elements of this system are connected in a closed circuit in which the air can circulate by the aid of a micropump placed in the aluminium flask. In the circuit there are also a flow-meter, a manometer and an hygrometer.

The system is calibrated using some bubblers (GRG) containing a Ra-226 reference solution of known activity (about 1500 Bq), referred to a NIST standard (National Institute of Standard and Technology, USA). The radon activities of the sources are in equilibrium with those of the radium sources. The GRG containing the radium solution is put in position n°2 (see Figure 2.1), while the GRG in the position n° 1 humidifies the air and avoid that the radium source dries. The circulation of the air through the GRG extracts the radon from the radium source and forces it into the circuit, giving rise to a radon reference atmosphere, i.e., an ambient where the radon concentration value is known. In fact, the radon activity is known, being in equilibrium with the radium activity, and the volume of the circuit is carefully measured. The efficiency of the monitor is thus simply evaluated comparing the count rate of the monitor with the value of the radon activity concentration. The result of a typical measure is showed in Figure 2.2.

Two INMRI monitors, an Alphaguard and a MR1, have been calibrated independently in this circuit and then compared in more than 25 experiments in the 1027 liters INMRI radon chamber. On average, their measurements were perfectly coincident, but in some cases a slight difference appeared; however, the standard deviation of the whole measurements was quite low: about 1.5%. This value represents the reproducibility limit of the radon measurements for this kind of instruments.

2.2 The control of the primary system

The most critical part of the calibration system is the stability of the radium sources and the difficulty of extracting the whole radon gas in equilibrium with radium. In order to control this aspects we used two different kind of radon sources whose activity were measured with “absolute methods”. The first source consist of a vial containing about 2 kBq of radon, measured in a NaI well detector (γ spectrometry measurements in 4π geometry). The second source was a GRG, whose volume was about 300 cm³, containing water with very high radon concentration, measured by means of a liquid scintillation detectors. The results of these experiments gave an agreement with those based on the GRG radium within the 1.2 %.

2.3 Effects of the density of the air

The parameter that has the greater influence on the response of the commonly used monitors is the density of the air, i.e., the ratio P/T, where P is the atmospheric pressure (in mBar) and T is the absolute temperature (K). For that reason, a number of measurements were performed in order to calculate the correction factors to be used when the monitors work in different density conditions. These corrections, generally negligible at normal laboratory conditions, have been quite relevant in Lurisia and cannot be generally ruled out in the field. For these kinds of experiments, an AG and a MR1 monitors were put in a 141 litres radon chamber; some radon was added and then the pressure was slightly decreased until a value of 110 mBar. 24 hours later, the pressure was restored to the initial (normal) level adding some “aged air” (with no radon) and the measurements continued for 24 hours. The results obtained from these experiments are shown in Figure 2.3.

We can see that the AG efficiency decreases as the density of the air decreases while for the MR1 the opposite applies. These facts can be easily explained considering that AG is based on an ionisation chamber where the ionisation is proportional to the quantity of the atoms in a volume (the density); by contrast, for the MR1, being based on a scintillation detector, the density decrease allows more α particles to reach the wall of the detector.

The results of these measurements are reported in Figure 2.4. In the environmental condition of Madame Curie’s Tunnel (931 mBar e 11°C), the Alphaguard monitors underestimated the real radon concentration of about 2.5%, while the MR1 monitors overestimated them of about 1.7%. For those reasons, all the measurement performed in Madame Curie’s Tunnel were corrected in order to take into account for these effects.

2.4 The calibration of the monitors used during the Lurisia intercomparison

All the monitors used during the Lurisia intercomparison have been calibrated comparing their responses with those of the INMRI reference monitors: a number of 13 comparison measurements were made. Three measurements have been performed in the 1027 litres radon chamber, at three different constant radon concentrations: 1500, 9000 e 25000 Bq/m³. The other measurements have been done in larger chamber, the “walkable radon chamber” (SRP), with variable radon concentrations in the range 1500 - 4000 Bq/m³. In Figure 2.5 it can be seen the experimental arrangement for a typical calibration in a SRP chamber while in Figure 2.6 the results of one of these measurements are shown.

The experiments made in the walkable radon chamber (SRP) showed that the radon levels can vary up to the 4% at a distance of 1.5 m. In general, the measurements in SRP radon chamber seem by far less reproducible than those performed in a standard radon chamber: however, we think that these results are more reliable for our purposes, being the SRP conditions closer to the in the field conditions. Each one of the monitors has been tested for at least 5 times; the reproducibility of the calibration factor resulted 1.7% for one MR1 detector and 2.4% for all the others. The overall uncertainty of the calibration factor of the monitors was thus estimated in the order of 3%.

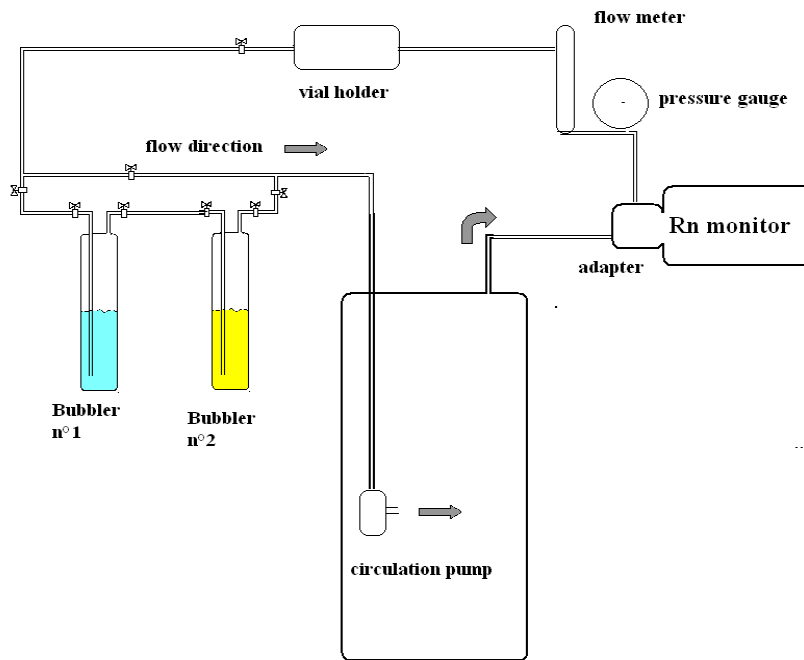


Figure 2.1. Scheme of the primary circuit for radon measurements in air.

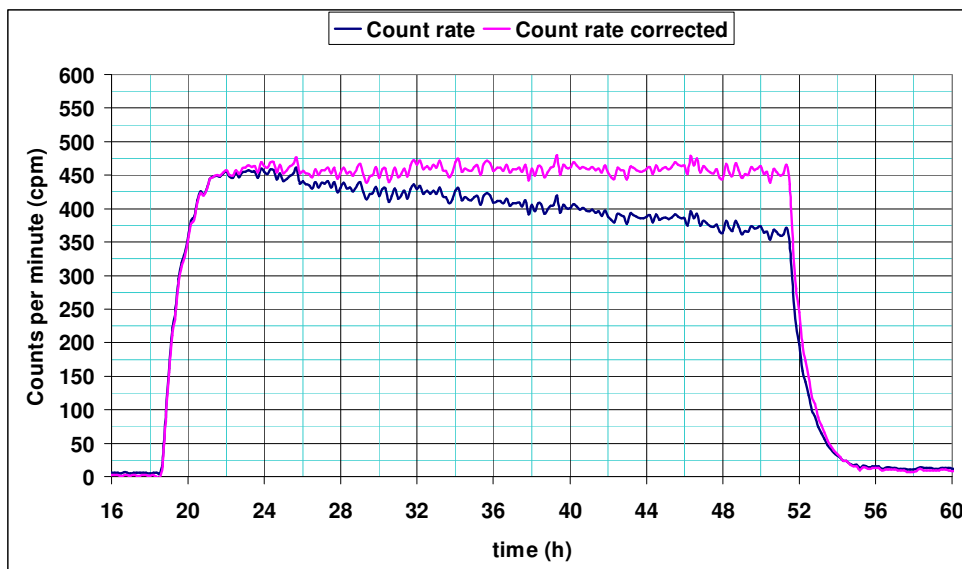


Figure 2.2. Example of a calibration measurement in the primary system.

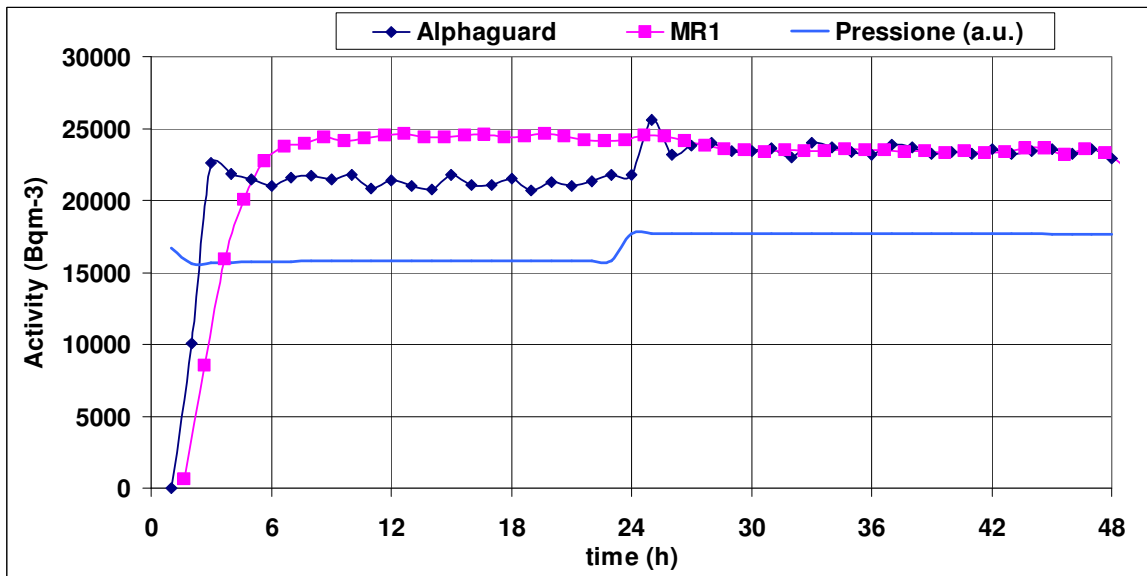


Figure 2.3. Measurement of the pressure effect on radon monitors response.

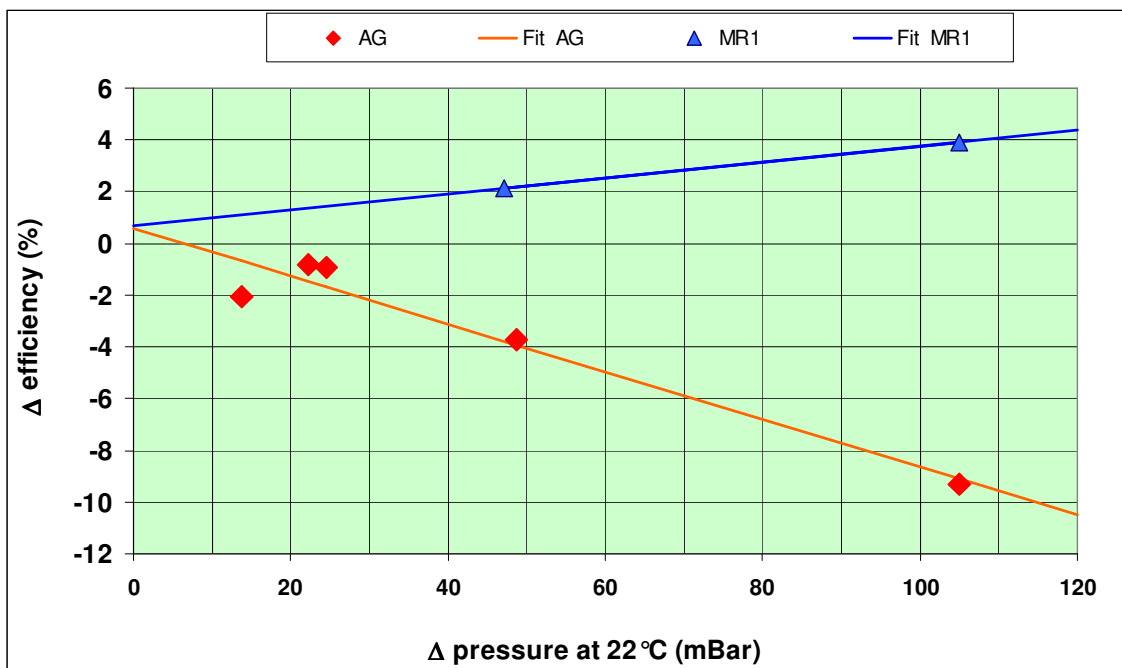


Figure 2.4. Variation of the efficiency of the monitors as a function of the variation of the air density.



Figure 2.5. Calibration of the monitors in the “radon walkable chamber” (SRP).

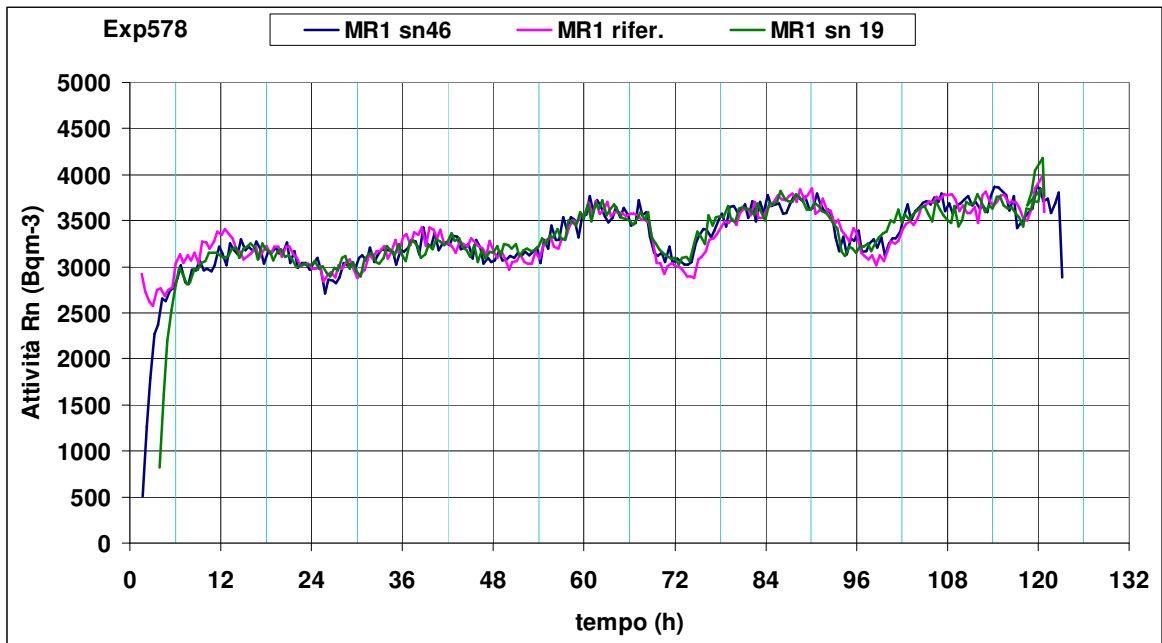


Figure 2.6. Measurements for calibration of the monitors in the “walkable radon chamber” (SRP).

3. The Lurisia Tunnel: characterisation of the site

3.1 Radiometric characterisation

The Lurisia Cave consists of a main Tunnel where there are some plants for collecting the water of the springs. One of these springs, the “Garbarino spring” is highly radioactive, up to 25000 Bq/l of radon. Twenty meters away from the entrance of the Tunnel, on the right, it opens a small cavity, where there is one of the main Garbarino wells. That site was chosen as the location for the intercomparison exposures: besides the very high radon concentration levels, the air circulation is low and the other environmental parameters (temperature and humidity) are quite stable. In this cavity, approximately 5 meters long, 3 meters wide and with an average height of 1.8 meters, 8 wire shelves were placed (see Figure 3.1: the shelves are identified with the letters from A to H) in order to assure a good air circulation between the dosimeters during the exposures.

During the weeks before the beginning of the intercomparison, 9 radon continuous monitors were placed on the shelves (Alphaguard, MR1, e Radim 5B, see Figure 3.2), six of which calibrated by INMRI, the others aligned with the previous ones through proper intercomparisons. These measurements allowed to verify the absence of any significant radon concentration gradient along the y (y: 0-80 cm) and the z axis (z: 0-100 cm; see Figure 3.1). A very clear gradient was observed instead for the x axis, especially during one of the two intercomparison exposures (the highest one, see Figure 3.4). The radon concentration in the days before the exposures showed a regular behaviour, with typical daily fluctuations (Figure 3.5): the radon concentrations decrease in night-time and increase during the day (Figure 3.6). The mean value of the day maxima resulted in 15272 Bq/m³, while the mean of the day minima was 6447 Bq/m³. During these tests, the highest maximum value of the radon concentration was 23936 Bq/m³, the lowest being 5696 Bq/m³. The highest minimum value was 16000 Bq/m³ while the minimum was 1536 Bq/m³.



Figure 3.1. The shelves where the dosimeters were placed during the intercomparison: the Cartesian reference system allows to trace the position of the dosimeters sets.

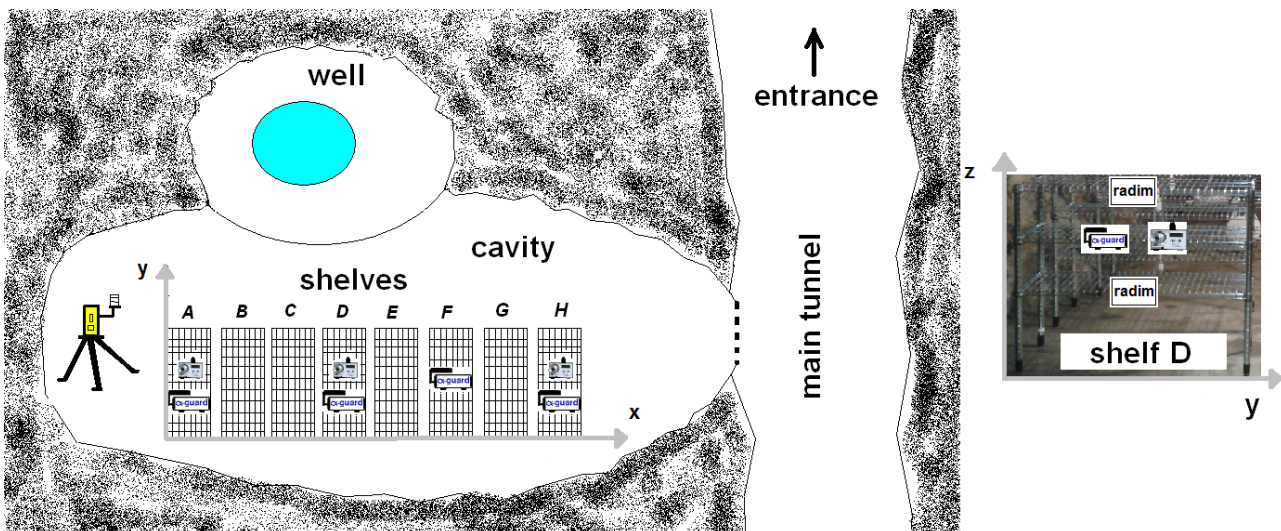


Figure 3.2. Scheme of the arrangement of the monitors during the exposures. A detailed picture of shelf D is shown on the right.

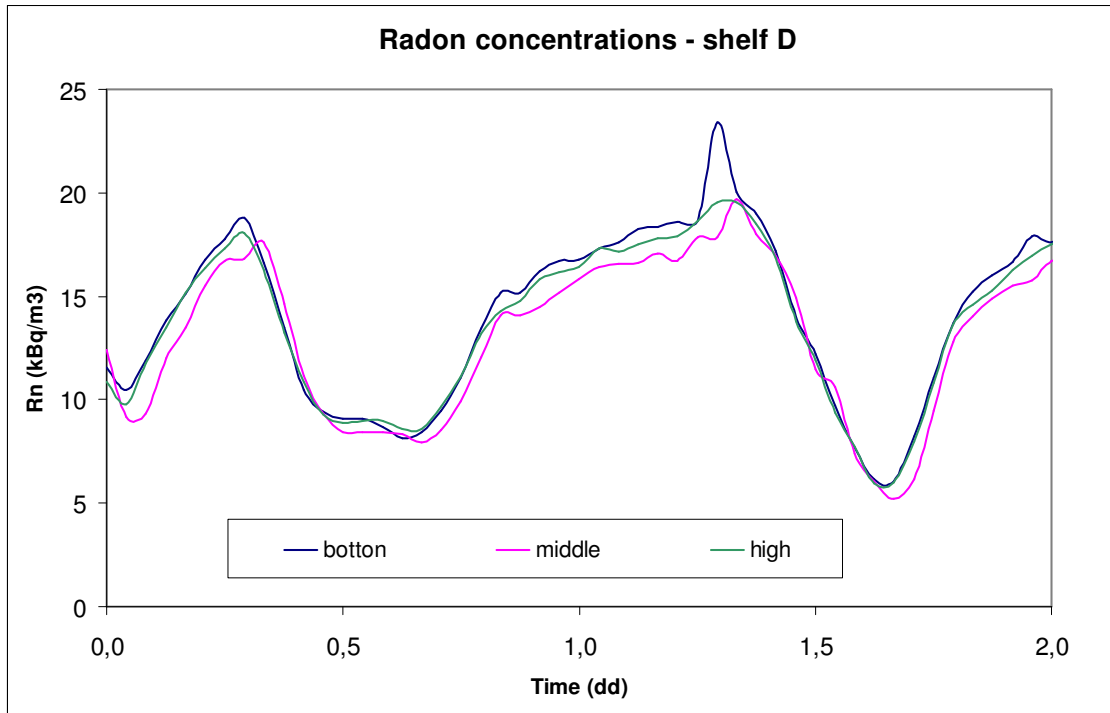


Figure 3.3. Typical radon concentration behaviour (monitors placed on the shelf D): the curves refer to different heights (z axis): black-bottom, red-middle, green-high.

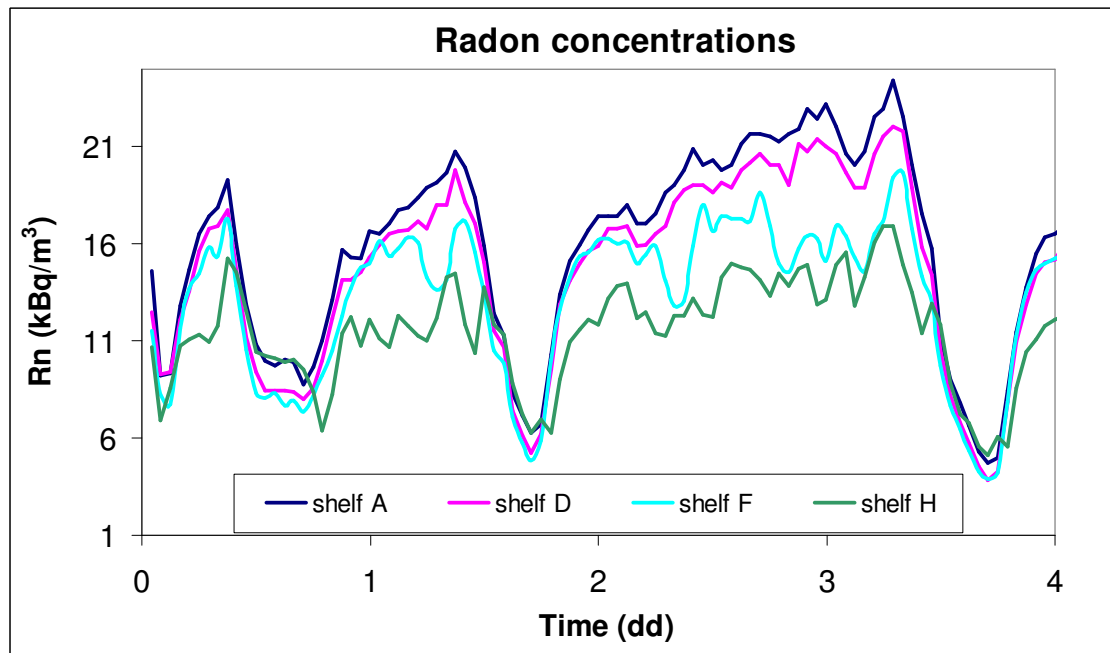


Figure 3.4. Radon concentration values for different shelves; as each shelf is identified by a different x axis value, this graph clearly show a gradient along the x coordinate.

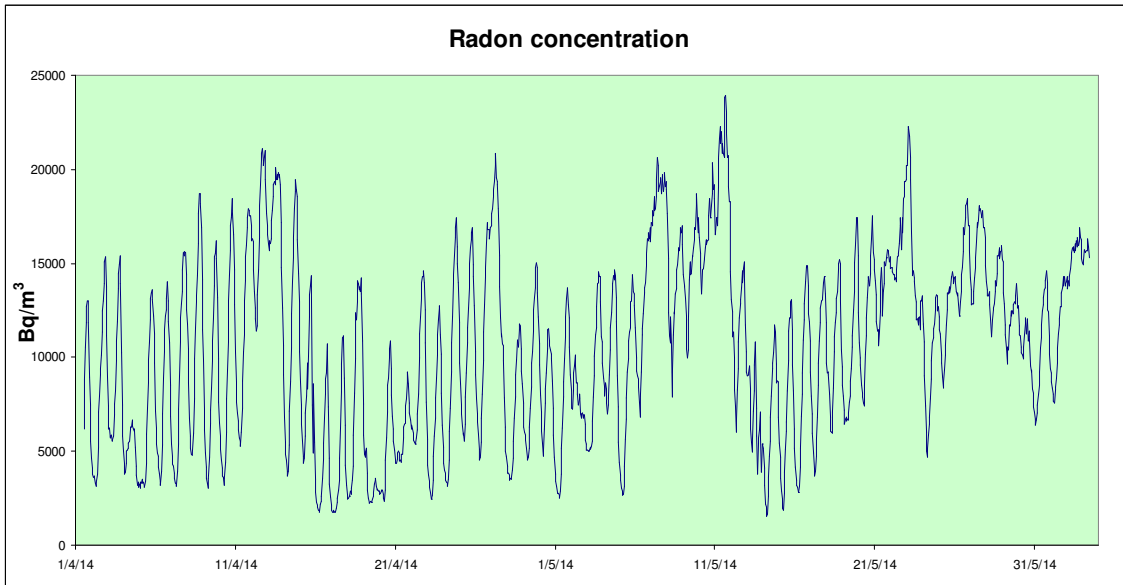


Figure 3.5. Radon measurements in the cavity before the beginning of the exercise

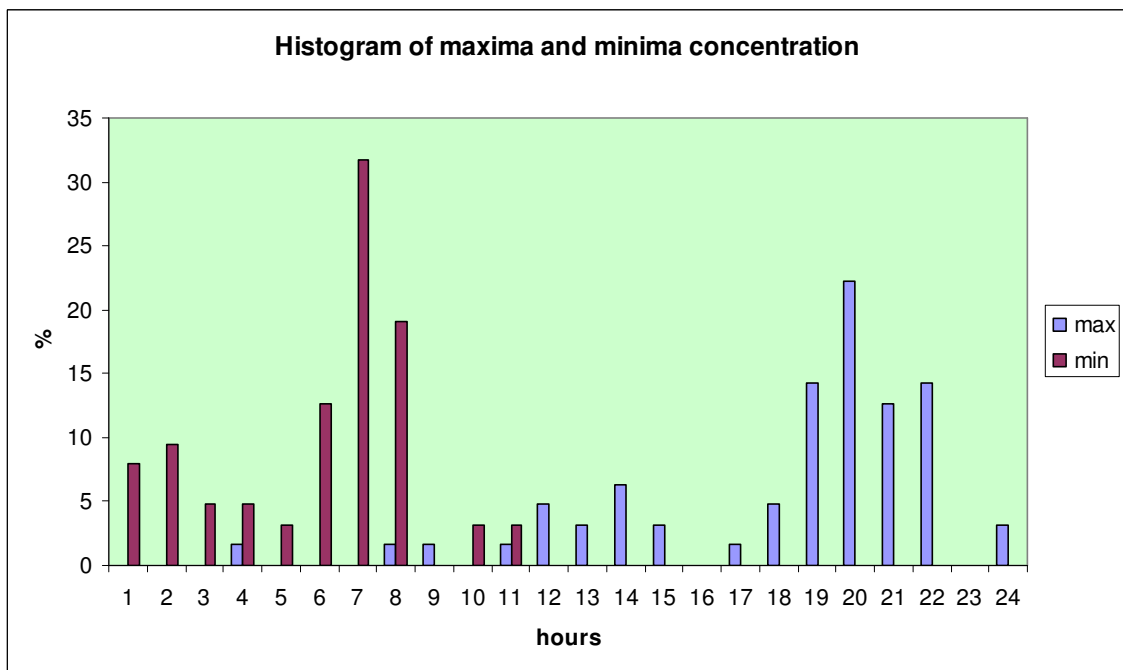


Figure 3.6. Istogram of daily maxima and minima in the intercomparison cavity

The gamma dose rate values in the measurement site has been evaluated by means of a plastic scintillator detector “Automess”. The radiation field in the volume occupied by the shelves was then calculated by the interpolation of the experimental data using as weights the $1/r^2$ function, with the software package R (Figure 3.7) [2]. It can be noticed that the radiation field is not uniform, probably because of the complex morphology of the cavity itself.

During the intercomparison exposures, the radiation field occupied by the shelves was evaluated by means of a set of thermoluminescence dosimeters (TLD-100): in this way it was then possible to assign to each dosimeters set a proper gamma dose rate value (see table 3.1).

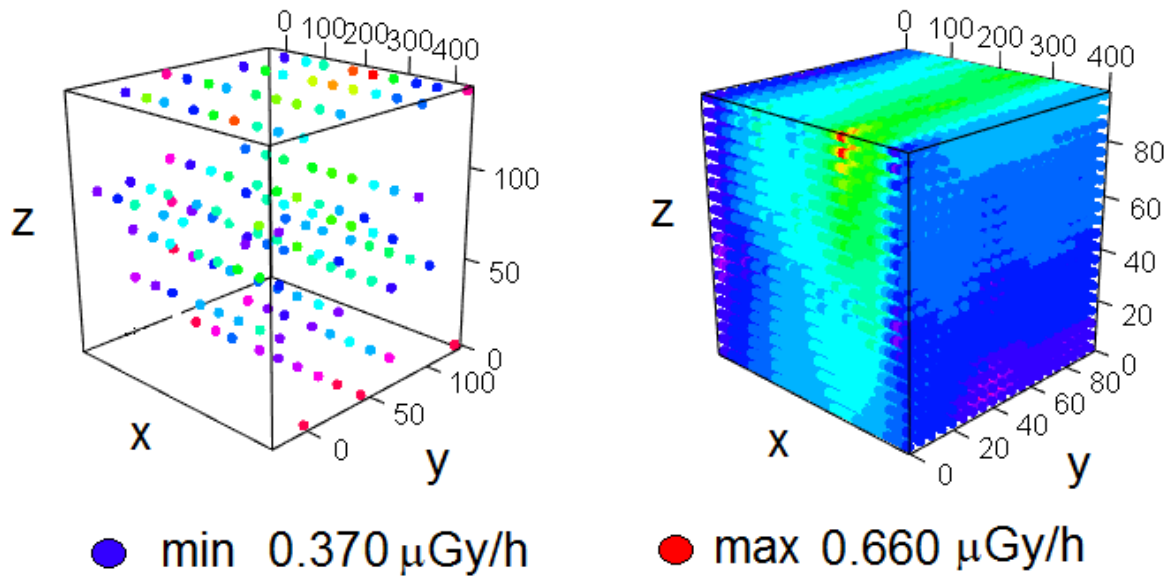


Figure 3.7. Gamma dose rate in air (experimental data) and evaluation of the radiation field.

Table 3.1 - γ dose rate in air for each dosimeters SET during the exposures

SET	Low exposure					High exposure				
	x cm	y cm	z cm	Dose rate $\mu\text{Gy/h}$	inc k=1 $\mu\text{Gy/h}$	x cm	y cm	z cm	Dose rate $\mu\text{Gy/h}$	inc k=1 $\mu\text{Gy/h}$
1	17	8	93	0,458	0,039	17	12	93	0,671	0,060
2	17	42	93	0,475	0,040	17	40	93	0,667	0,060
3	17	66	93	0,494	0,042	17	63	93	0,687	0,062
4	17	33	40	0,458	0,039	17	43	40	0,656	0,059
5	17	70	40	0,475	0,040	17	74	40	0,664	0,060
6	90	43	93	0,482	0,041	90	46	93	0,657	0,059
7	73	24	93	0,472	0,040	73	19	93	0,639	0,057
8	73	60	93	0,490	0,042	73	42	93	0,658	0,059
9	73	26	67	0,467	0,040	73	49	67	0,662	0,060
10	73	24	40	0,457	0,039	73	20	40	0,616	0,055
11	73	63	40	0,476	0,040	73	60	40	0,665	0,060
12	118	30	93	0,486	0,041	118	30	93	0,637	0,057
13	118	55	93	0,489	0,042	118	70	93	0,673	0,061
14	118	21	67	0,484	0,041	118	25	67	0,627	0,056
15	118	50	67	0,483	0,041	118	43	67	0,641	0,058
16	118	24	40	0,473	0,040	118	30	40	0,622	0,056

SET	Low exposure					High exposure				
	x cm	y cm	z cm	Dose rate $\mu\text{Gy/h}$	inc k=1 $\mu\text{Gy/h}$	x cm	y cm	z cm	Dose rate $\mu\text{Gy/h}$	inc k=1 $\mu\text{Gy/h}$
17	118	50	40	0,478	0,041	118	62	40	0,644	0,058
18	118	75	67	0,479	0,041	118	76	67	0,660	0,059
19	190	20	93	0,487	0,041	190	20	93	0,626	0,056
20	190	70	93	0,541	0,046	190	76	93	0,683	0,061
21	237	30	93	0,497	0,042	237	36	93	0,615	0,055
22	237	65	93	0,502	0,043	237	70	93	0,645	0,058
23	237	25	67	0,496	0,042	237	18	67	0,598	0,054
24	237	50	67	0,494	0,042	237	53	67	0,622	0,056
25	237	75	67	0,492	0,042	237	80	67	0,637	0,057
26	237	40	40	0,487	0,041	237	32	40	0,598	0,054
27	237	70	40	0,483	0,041	237	72	40	0,619	0,056
28	284	20	93	0,497	0,042	284	10	93	0,598	0,054
29	284	38	93	0,489	0,042	284	38	93	0,601	0,054
30	284	70	93	0,492	0,042	284	70	93	0,628	0,056
31	284	55	40	0,476	0,040	284	55	40	0,597	0,054
32	264	43	50	0,485	0,041	266	50	40	0,602	0,054
33	284	73	67	0,481	0,041	284	76	67	0,621	0,056
34	334	25	93	0,475	0,040	334	28	93	0,574	0,052
35	334	13	93	0,483	0,041	334	10	93	0,577	0,052
36	334	43	93	0,470	0,040	334	42	93	0,577	0,052
37	334	70	93	0,469	0,040	334	66	93	0,591	0,053
38	334	74	67	0,454	0,039	334	20	67	0,568	0,051
39	334	13	67	0,481	0,041	334	40	67	0,571	0,051
40	334	32	67	0,469	0,040	334	56	67	0,576	0,052
41	334	47	67	0,464	0,039	334	66	67	0,580	0,052
42	334	36	40	0,461	0,039	334	43	40	0,565	0,051
43	334	56	67	0,461	0,039	334	80	67	0,582	0,052
44	334	65	40	0,450	0,038	334	74	40	0,567	0,051
45	334	12	40	0,461	0,039	334	15	40	0,550	0,049
46	378	12	93	0,432	0,037	378	20	93	0,528	0,048
47	378	35	93	0,448	0,038	378	48	93	0,551	0,050
48	378	67	93	0,452	0,038	378	75	93	0,551	0,050
49	378	30	40	0,433	0,037	378	10	40	0,471	0,042
50	378	12	40	0,403	0,034	361	52	40	0,548	0,049

3.2 Environmental monitoring

All participants received the information about all the relevant environmental data (see Table 3.2), referred to the two intercomparison exposures. The meteorological and climatic data (temperature, pressure and humidity) were gathered by an Automatic Weather Station MAWS201 (Vaisala). The Station acquired the data every 60 seconds and calculated the hourly means. The pressure values are affected by an uncertainty of $\pm 0.3\text{hPa}$; the

humidity values (at +20°C), ± 2 %RH (from 0 to 90%RH) and ±3 %RH (from 90 to 100%RH); the temperature values (at +20°C) di ±0.2 °C.

Table 3.2 Data sent to all the participants

	Low exposure	High exposure
Height (above sea level) of the exposure site	720 m a.s.l.	
Height (above sea level) of the storing place of the dosimeters (Ivrea, Arpa Piemonte Lab.)	253 m a.s.l.	
Gamma dose rate of the storing place	0.150 ± 0.015 µGy/h (k=1)	
Time of exposure	46 ore	382 ore
Temperature	9.3°C	9.2°C
Pressure	931.8 hPa	930.8 hPa
Humidity %	94.8	94.5

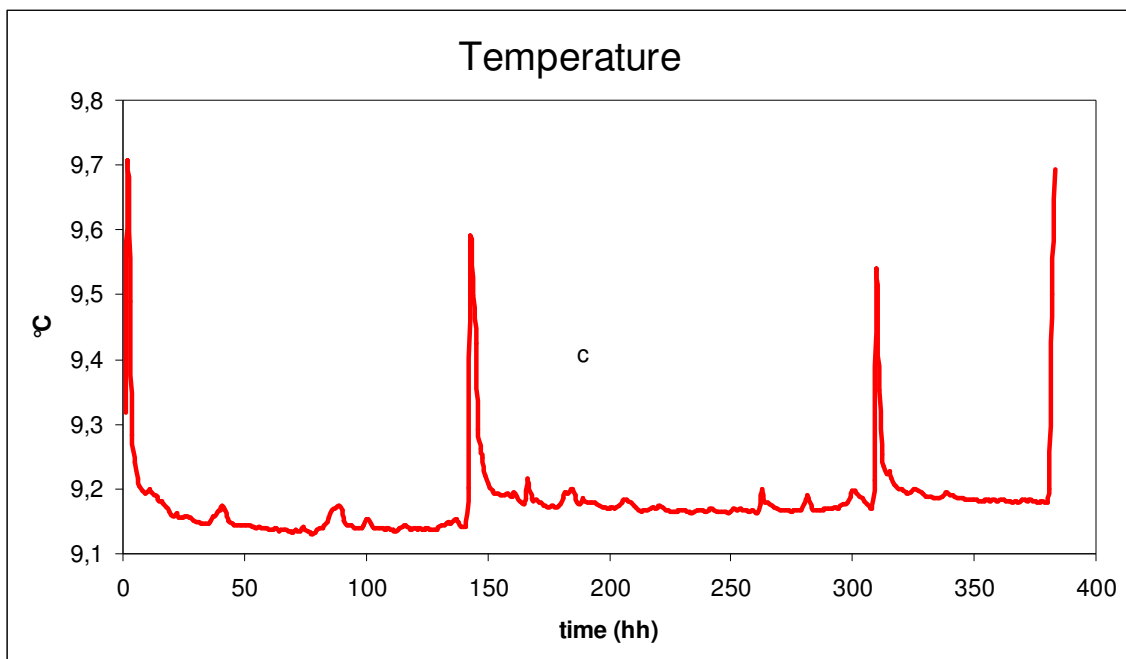


Figure 3.8. Temperature variation during the high exposure.

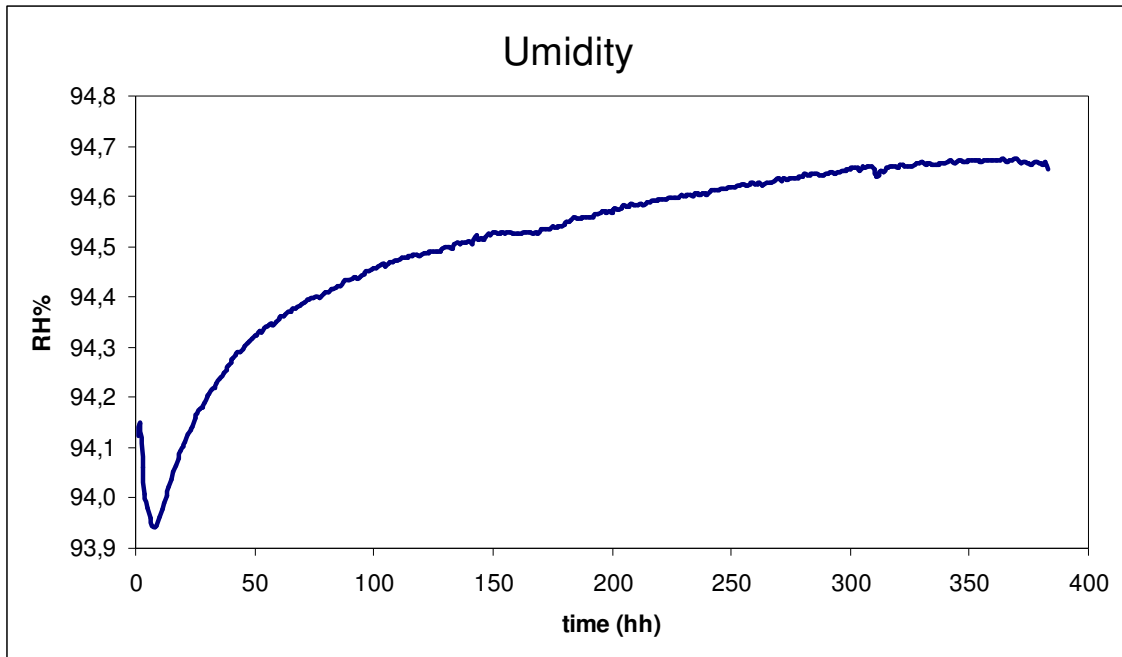


Figure 3.9. Humidity variation during the high exposure.

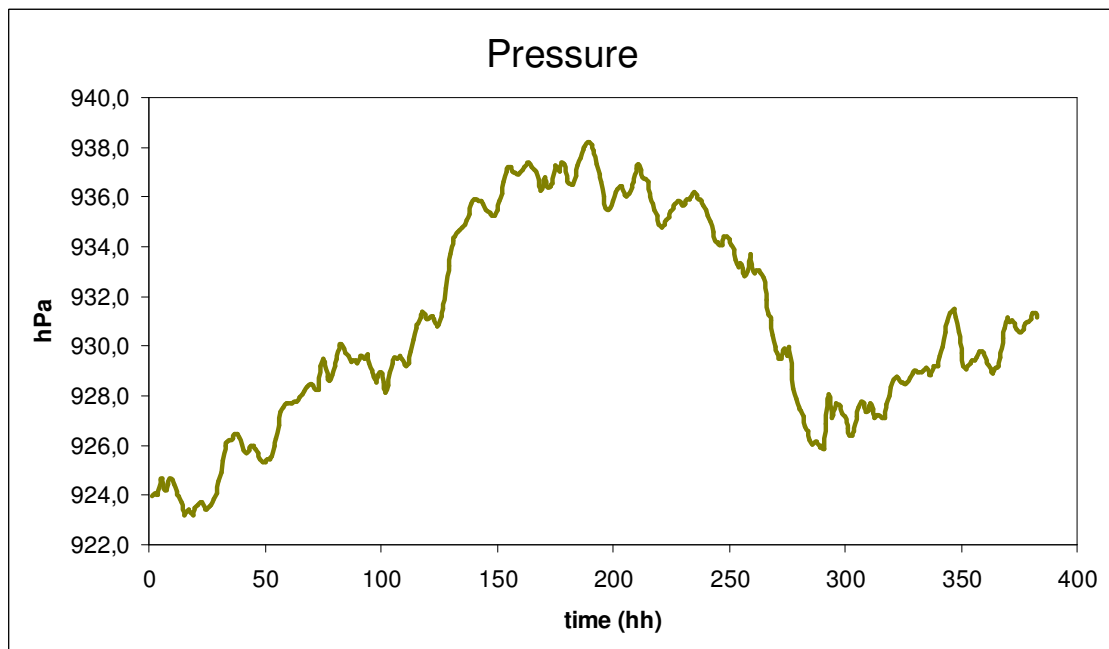


Figure 3.10. Pressure variation during the high exposure.

4. Logistics and evaluation of the exposures

Several days before the beginning of the exposures, the reference monitors were placed in the Lurisia Tunnel in order to avoid any response delay of the instruments at the starting of the intercomparison exercise. The participants sent us two groups of dosimeters (10 dosimeters each), one for a low exposure (around 400 kBqhm⁻³), the other for a high exposure (about 8000 kBqhm⁻³).

All the dosimeters has been previously stored at Arpa Piemonte Laboratory (Ivrea) in their radon proof envelope, until the day before the beginning of the exposures. The envelopes were then opened only for the limited time needed for the arrangement of the dosimeters (following the indications given by each participant) and then sealed again.

After reaching Lurisia, the sets were placed in boxes (Figures 4.1 e 4.2), before the entrance of the Tunnel. From that moment the transits (two dosimeters for each group) have been separated from the other dosimeters. The positioning of the dosimeters on the shelves inside the Tunnel took no more than 10 minutes (Figura 4.3).

The two exposures were performed in sequence: the first was the higher one, the second the lower. During the exposures of the dosimeters, the radon concentration in the Tunnel was controlled checking periodically the reference monitors.

At the end of the exposures all the dosimeters, together with the transits, were collected and stored in an outdoor place in Ivrea for several days, before being sealed again in radon proof bags. The schedule of the exposures is shown in the following tables 4.1 and 4.2.

Table 4.1 Schedule of the exposure of the dosimeters - low value

Beginning of the storing (Ivrea)	End of the storing	Start of the exposure	End of the exposure	End of the outdoor storing	End of storing in Ivrea - Shipping
Arrival date of the dosimeters	5/8/2014 16:00	6/8/2014 14:00	8/8/2014 12:00	13/8/2014 11:00	3/9/2014

Table 4.2 Schedule of the exposure of the dosimeters - high value

Beginning of the storing (Ivrea)	End of the storing	Start of the exposure	End of the exposure	End of the outdoor storing	End of storing in Ivrea - Shipping
Arrival date of the dosimeters	9/7/2014 8:00	9/7/2014 15:00	25/7/2014 13:00	5/8/2014 9:00	3/9/2014



Figure 4.1. Opening of the radon proof bags outside the Lurisia Tunnel.



Figure 4.2. Preparation of the sets before the entrance to the Tunnel.

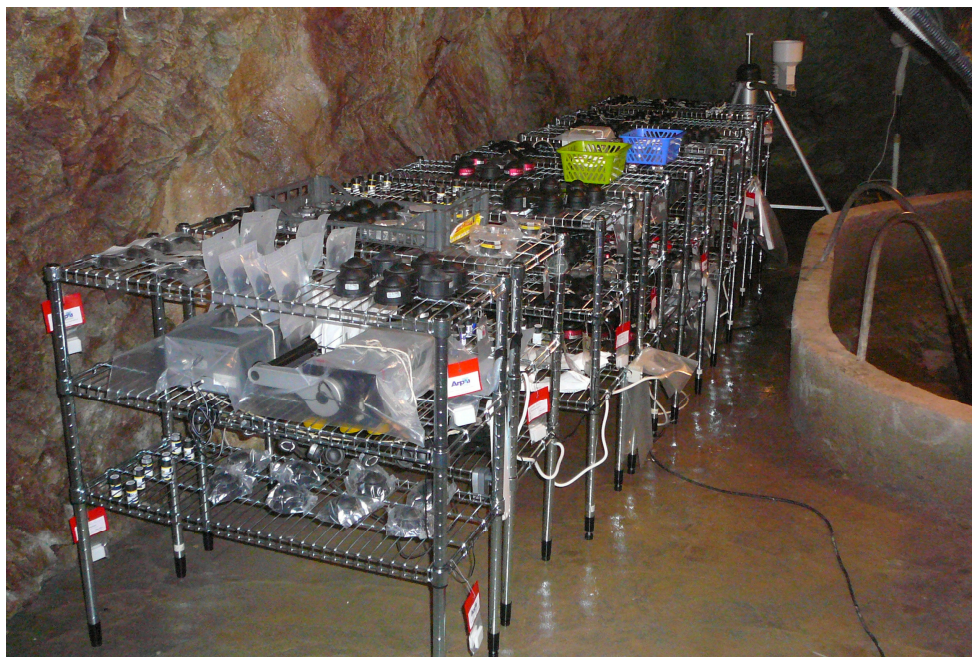


Figure. 4.3. The dosimeters on the shelves during the exposure.

In order to give a reference radon exposure value for each set, have been considered only the monitors calibrated at INMRI, placed on the shelves A, D e H. Taking the data acquired by these monitors, the INMRI determined the reference values (see tables 4.3, 4.4) and the related uncertainties (4% for the high exposure, 5% for the low exposure). The INMRI certificates are available in the Annexes 1 and 2.

Table 4.3 – Reference values for the low exposure as a function of the position (x axis value)

Shelf	X cm	Reference Value kBqh/m ³	unc (k=1) kBqh/m ³
A	0	616	31
D	173	595	30
H	369.5	613	31

Table 4.4 - Reference values for the high exposure as a function of the position (x axis value)

Shelf	X cm	Reference Value kBqh/m ³	unc (k=1) kBqh/m ³
A	0	8712	348
D	173	8167	327
H	369,5	6029	241

Two quite different situations appear for the two exposure levels.

For the low exposure level (Figure 4.4) no statistically significant variation along the three axis x,y,z, was found. Therefore a unique reference value for all the sets exposed has been established, simply averaging the three experimental data of table 4.3: 608 ± 74 ($k=2$) kBqhm^{-3} (Figure 4.5). On the contrary, for the high exposure level, a significant variation along the x axis was observed. In this case, the reference value for each set was therefore evaluated fitting the experimental data (Table 4.4) with a second degree polynomial (Figure 4.7). It was thus possible to obtain the reference levels for all the exposed sets simply knowing the value of the corresponding x coordinate (Table 4.5). The calculated exposure levels were in the range $5900 - 8714 \text{ kBqhm}^{-3}$. The uncertainty of the reference value for each set was evaluated taking into account three different contributions: the uncertainty of the measurement estimated by INMRI, the uncertainty due to the interpolation and a third contribution due to the uncertainties related to the exposure time and the position of the sets on the shelves. The overall uncertainty on the reference values was thus estimated in the range 4.5 - 5% for the high exposure and 6% for the low exposure.

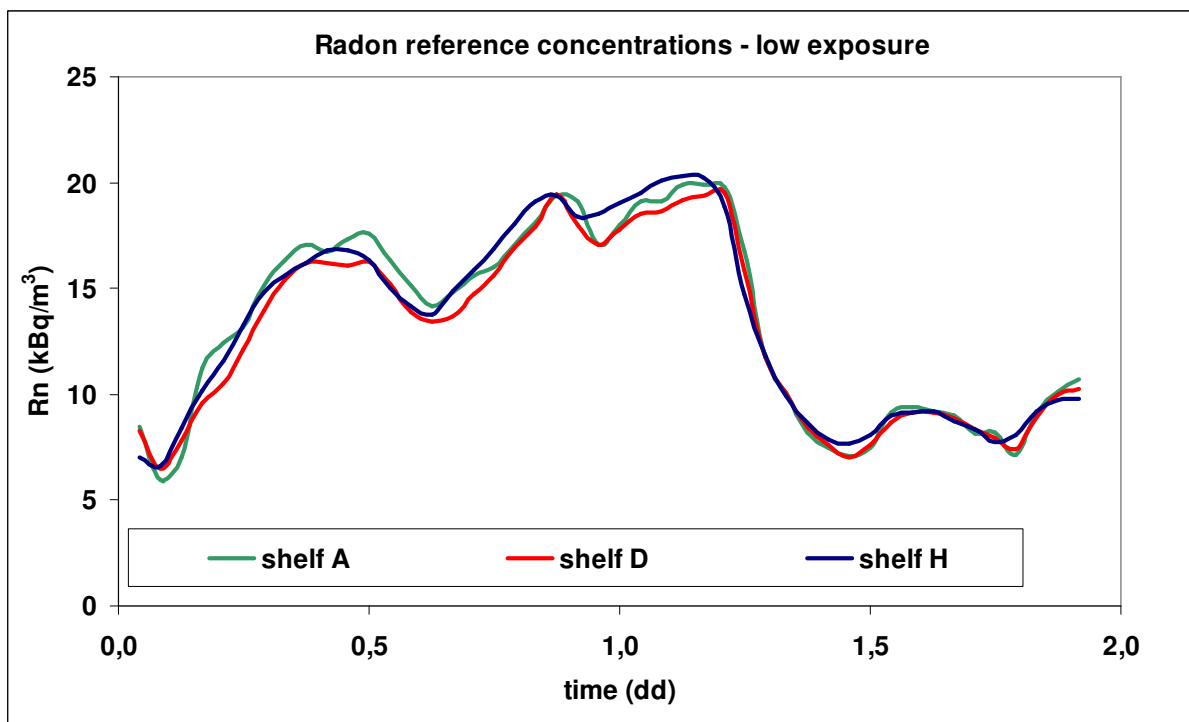


Figure 4.4. Radon levels (reference monitors) during the low exposure.

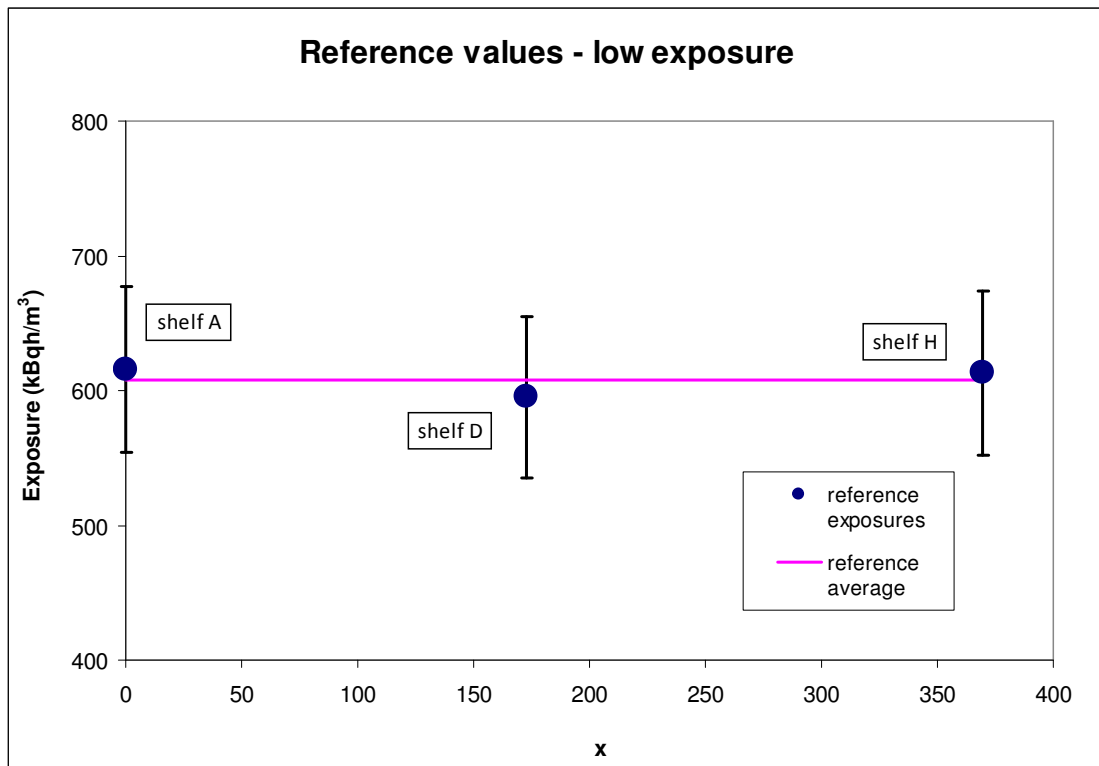


Figure 4.5. Low exposure experimental reference values and average reference value.

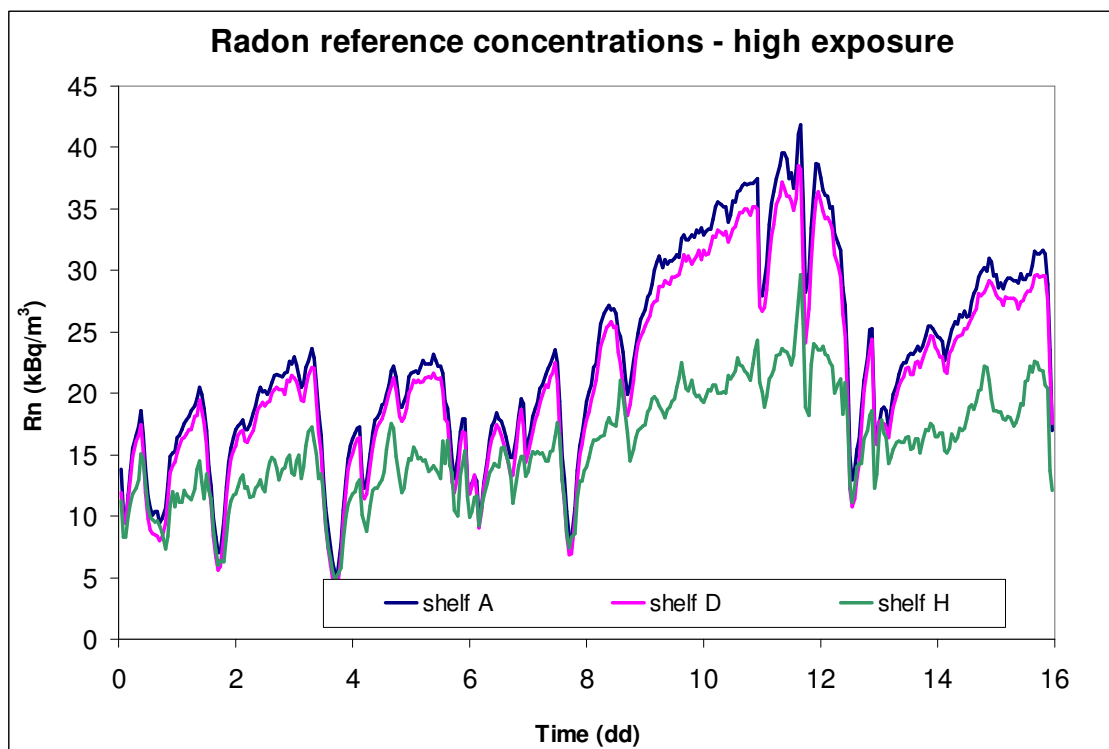


Figure 4.6. Radon concentration (reference monitors) during the high exposure.

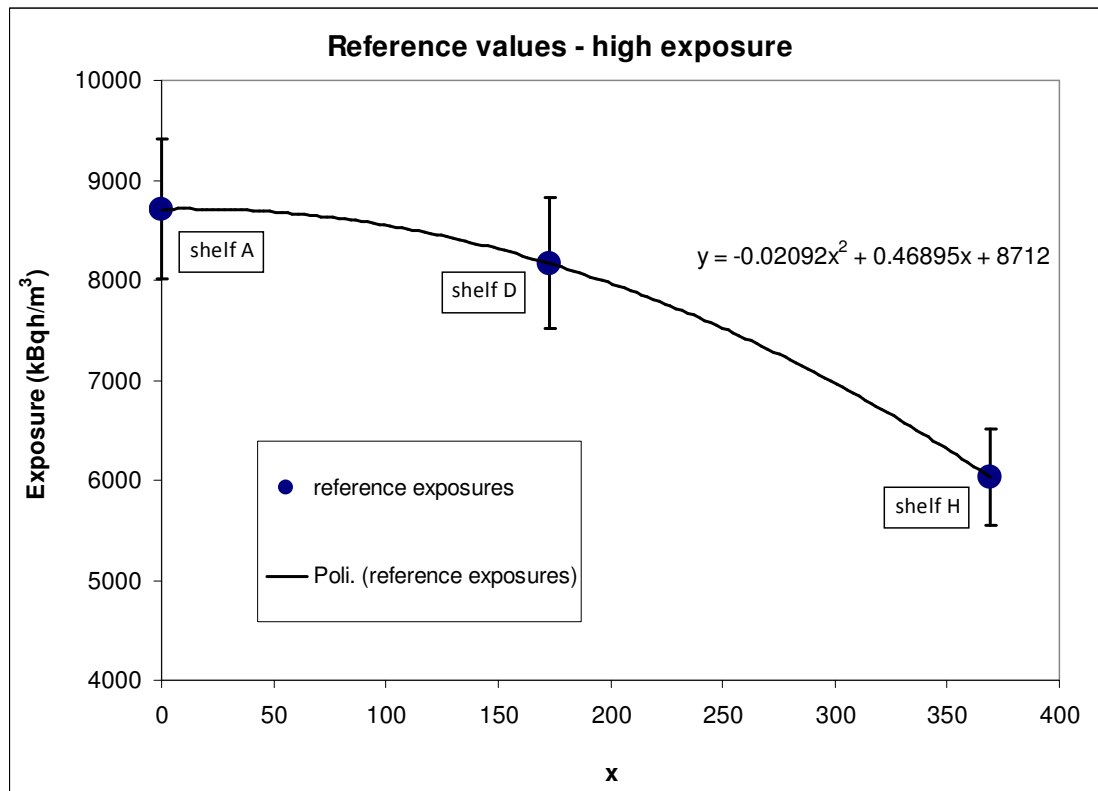


Figure 4.7. High exposure experimental reference values and the polynomial interpolation

Table 4.5 - Reference values for the high exposure for each dosimeters set

SET	X cm	Reference Value kBqh/m ³	Unc. (k=2) kBqh/m ³
1	17	8714	788
2	17	8714	788
3	17	8714	788
4	17	8714	788
5	17	8714	788
6	90	8585	832
7	73	8635	833
8	73	8635	833
9	73	8635	833
10	73	8635	833
11	73	8635	833
12	118	8476	807
13	118	8476	807
14	118	8476	807
15	118	8476	807
16	118	8476	807
17	118	8476	807
18	118	8476	807

SET	X cm	Reference Value kBqh/m³	Unc. (k=2) kBqh/m³
19	190	8046	729
20	190	8046	729
21	237	7648	746
22	237	7648	746
23	237	7648	746
24	237	7648	746
25	237	7648	746
26	237	7648	746
27	237	7648	746
28	284	7158	704
29	284	7158	704
30	284	7158	704
31	284	7158	704
32	266	7357	730
33	284	7158	704
34	334	6535	590
35	334	6535	590
36	334	6535	590
37	334	6535	590
38	334	6535	590
39	334	6535	590
40	334	6535	590
41	334	6535	590
42	334	6535	590
43	334	6535	590
44	334	6535	590
45	334	6535	590
46	378	5900	528
47	378	5900	528
48	378	5900	528
49	378	5900	528
50	361	6155	563

5. Results and discussion

5.1 Presentation of the data

The laboratories which took part to this exercise were 46, 34 of them coming from Italy and 12 from other different countries (3 from Spain, 2 from France and 1 from Germany, Austria, Albania, Slovenia, Sweden, Turkey and Argentina). A total number of 50 sets were sent to the organisers: in fact 4 laboratories sent a double quantity: 4 sets of dosimeters each. Seven laboratories out of the 46 are resulted accredited ISO17025. The detailed list of all the participants is reported in Table 5.1.

Most of the devices sent were dosimeters equipped with CR39 detectors (32), then electrets (12), dosimeters with LR115 (5) and Makrofol (1).

The results we received refer to 48 of the 50 sets exposed in the Lurisia Tunnel. Laboratory ID10 gave precise results only for the low exposure (for the high exposure gave a lower limit, $> 5000 \text{ kBqhm}^{-3}$), while laboratory ID27 gave lower limits in both cases: >369.6 and $>4106 \text{ kBqhm}^{-3}$. For those reasons these laboratories have been disregarded in the following discussion.

In some cases the radon exposure value was given as a net value, ie. with the transit contribution already subtracted: in these cases, of course, the transit values were not known and we took the data as they were. For all the others, we calculated the arithmetic mean of the two transits and we subtracted this value to each single dosimeter, thus obtaining the net value of the exposure.

From these net values we calculated the arithmetic mean and the median; in most cases the values of these two parameters were very close, showing thus a roughly symmetric distribution of the data.

In Figure 5.1 the results referred to the low exposure are shown: for each laboratory the arithmetic mean $\langle E \rangle$ and the standard deviation S_E are reported. The solid line represents the reference value E_R for the exposure, in this case 608 kBqhm^{-3} , while the grey lines are the related uncertainty. The plot shows that most of the laboratories gave results in good agreement with the reference value, even if, as a whole, a slightly underestimation trend appears.

Similarly, in Figure 5.2 the results for the high exposure are reported. In this case, however, we do not have a single reference value E_R but several, in the range $5900 - 8714 \text{ kBqhm}^{-3}$.

In the Tables 5.2 and 5.3 a more comprehensive presentation of the data are shown: in particular, besides the reference values E_R , the laboratory arithmetic mean $\langle E \rangle$ and the standard deviation S_E we report also the standard composite uncertainty SL (associated to the series of the n instrumental readings and related to $n - 1$ degree of freedom) and other statistical parameters defined as follows:

The REF

$$REF = \frac{\langle E \rangle}{E_R}$$

The trueness:

$$trueness = \frac{\langle E \rangle - E_R}{E_R}$$

The precision:

$$precision = \frac{S_E}{\langle E \rangle}$$

The normalized error E_n :

$$E_n = \frac{\langle E \rangle - E_R}{\sqrt{U(E)^2 + U(E_R)^2}}$$

The z-score:

$$z = (\langle E \rangle - E_R) / \sigma_R$$

The quantity σ_R that appears in the z-score definition is the standard deviation chosen as a target for this exercise: in our case we decided to take for σ_R a value equal to the 20% of the reference value.

The absolute values of the z-score for both the low and high exposures, presented in the Tables 5.2 and 5.3, are also reported in Figures 5.3 and 5.4. Following the indication of the ISO/IEC 17043:2010 [4] and ISO 13528:2005 [5] the laboratories with z-score > 2 (absolute value) have been highlighted as their values cannot be considered fully acceptable. More precisely, following the ISO approach, a z-score in the range 2 - 3 shows that some measurement problems have to be solved, while a value greater than 3 is considered unacceptable. However, a large majority of laboratories (87%), showed a z-score < 2.

Table 5.1 List of participants

Laboratory	Conctat person	Country	Device	Detector
AGES Austrian Agency for Health and Food Safety	Wurm Gernot	Austria	RSKS	CR39
Algade - Francia	Pierre Filleul	Francia	DPR2	LR115
Appa TN - Settore Laboratorio (SL)	Mauro Bonomi, Stefano Pegoretti	Italia	E-PERM	Elettrete
Arpa FVG Udine	Silvia Pividore	Italia	RSK	CR39
Arpa Lazio - Servizio Agenti Fisici, sezione provinciale di Roma	Tommaso Aureli	Italia	RSKS	CR39
Arpa Lombardia - CRR Milano	Daniela Lunesu	Italia	TASL	CR39
ARPA Lombardia- Centro Regionale di Radioprotezione - sede di Bergamo	Silvia Arrigoni	Italia	RSKS	CR39
Arpa Sicilia Struttura Territoriale di Palermo	Antonio Sansone Santamaria	Italia	Radout	CR39
ARPA Umbria	Paola Sabatini	Italia	E-PERM	Elettrete
ARPA Valle di Aosta	Massimo Faure Ragani	Italia	ENEA-DISP	LR115
ARPAM - Dipartimento Provinciale di Ancona	Corrado Pantalone	Italia	E-PERM	Elettrete
Autoridad Regulatoria Nuclear of Argentina	Juan Pablo Bonetto	Argentina	KFK	CR39
CISAM	Raffaele Zagarella	Italia	RSKS	CR39
CRR Arpa Molise	Claudio Cristofaro	Italia	E-PERM	Elettrete
Dipartimento di Fisica - Università di Napoli Federico II - Lab Radioattività	Vincenzo Roca	Italia	Modello Anpa	LR115
Dipartimento di Fisica - Università di Napoli Federico II - Lab Radioattività	Vincenzo Roca	Italia	E-PERM	Elettrete
Dosirad	F Sarradino, F. Boudet, N Tharaud	Francia	DRF	LR115
ENEA IRP-DOS Bologna	Silvia Penzo	Italia	Enea -IRP	CR39
European Commission - Joint Research Centre Ispra Site Management - Nuclear Decommissioning Unit - Dosimetry Service	Andrea Ravazzani, Giacomo Maretti	Italia	Radout	CR39
FGM Ambiente sas	Luisa Salvatori	Italia	RSKS	CR39
I.N.F.N - Sezione di Torino	Michela Chiosso	Italia		CR39
INAIL - Consulenza Tecnica Accertamento Rischi e Prevenzione - Laboratorio di Igiene Industriale	Piero La Pegna	Italia	E-PERM	Elettrete
INFN - Laboratori Nazionali del Sud CATANIA	Stefano Romano	Italia	E-PERM	Elettrete
INFN Sez. Milano - Laboratorio LASA	Flavia Groppi	Italia		CR39

Laboratory	Conctat person	Country	Device	Detector
Institute of Applied Nuclear Physics, University of Tirana	Kozeta Tushe	Albania	NRPB/SSI	CR39
Istituto Nazionale di Fisica Nucleare - Dipartimento di Fisica Università di Catania	Immé Josette	Italia	Radout	CR39
Istituto Superiore di Sanità	Marco Ampollini	Italia		CR39
Lab. Chimico - radiochimico- ambientale Sogin	Pisciotta F., Casapulla K., Raulo Q.	Italia	RSKS	CR39
Lab. Fisico E. Majorana Arpacal Catanzaro	Procopio Salvatore	Italia	E-PERM	Elettrete
Lab. RI-RN DiMEILA- INAIL	Rosabianca Trevisi	Italia	NRPB/SSI	CR39
Laboratorio de radon de galicia -Universidad de Santiago de Compostela	Juan Miguel Barros - Dios	Spagna	RSKS	CR39
Laboratorio di Radioattività Ambientale (CIRCE), Dip. di Matematica e Fisica, Seconda Univ. degli studi di Napoli	Carlo Sabbarese	Italia	ANPA	CR39/LR115
Laboratorio Radiactividad Ambiental Universidad Politecnica de Valencia	Josefina Ortiz Moragon	Spagna	E-PERM	Elettrete
Landauer Nordic AB	Tryggue Ronnquist	Svezia	NRPB/SSI	CR39
LaRUC	Jose Luis Gultierrez Villanueva	Spagna		CR39
Lavoro e Ambiente srl	Giacomo Zambelli	Italia	RSKS	CR39
MCF Ambiente Srl	Silvia Gerardi	Italia	RSK	CR39
Mi.am srl	Antonio Parravicini	Italia	Radout	CR39
RADCHEM SRL	Aldo Cianchi	Italia	E-PERM	Elettrete
Radon Laboratory, Karlsruhe Institute of Technology	Ingo Fesenbeck	Germania	KIT	Makrofol
Saraykoy Nuclear Research Center - Health Pgysics Department, Radon Monitoring Lab.	Sefa Kemal Uzun, Isik Demiroz	Turchia	Radosys	CR39
Servizio di Radioprotezione dell'Università di Cagliari	Paolo Randaccio, Alessandra Bernardini	Italia		CR39
Universita' degli Studi di Torino - Servizio Centralizzato di Esperto Qualificato	Lorenzo Visca	Italia	E-PERM	Elettrete
U-Series Srl	Massimo Esposito	Italia	Radosure	CR39
X-Gammaguard di Laura Pini	Gianluca Troiano	Italia	RADOUT	CR39
X-Gammaguard di Laura Pini	Gianluca Troiano	Italia	E-PERM	Elettrete
ZVD Zavod za varstvo pri delu d.d. Institute of Occupational Safety	Peter Jovanovič	Slovenia	GAMMADATA	CR39

Table 5.2 Results - low exposure

Lab Code	E _R	⟨E⟩	S _E	SL%	REF	Trueness%	Precision%	En	z- score
1	608	643	28	7.8%	1.06	5.8%	4.7%	0.28	0.29
2	608	514	23	5.6%	0.84	-15.5%	3.8%	-1.01	-0.78
3	608	682	34	5.3%	1.12	12.1%	5.7%	0.71	0.61
4	608	1352	1452	36.5%	2.22	122.4%	238.8%	0.75	6.12
5	608	621	37	7.3%	1.02	2.1%	6.1%	0.11	0.10
6	608	478	114	9.3%	0.79	-21.5%	18.7%	-1.13	-1.07
7	608	652	29	6.8%	1.07	7.2%	4.7%	0.38	0.36
8	608	560	19	5.8%	0.92	-7.9%	3.2%	-0.49	-0.40
9	608	599	22	4.7%	0.99	-1.4%	3.6%	-0.09	-0.07
10	608	651	47	15.2%	1.07	7.0%	7.7%	0.20	0.35
11	608	698	21	1.3%	1.15	14.8%	3.4%	1.19	0.74
12	608	616	33	5.3%	1.01	1.3%	5.4%	0.08	0.06
13	608	181	130	25.4%	0.30	-70.3%	21.4%	-3.62	-3.51
14	608	462	30	9.0%	0.76	-24.0%	5.0%	-1.31	-1.20
15	608	463	28	9.0%	0.76	-23.9%	4.7%	-1.30	-1.19
16	608	548	23	3.8%	0.90	-9.9%	3.9%	-0.71	-0.50
17	608	299	106	19.7%	0.49	-50.8%	17.4%	-2.22	-2.54
18	608	372	51	20.0%	0.61	-38.8%	8.5%	-1.42	-1.94
19	608	581	26	5.4%	0.95	-4.5%	4.3%	-0.28	-0.23
20	608	545	111	19.6%	0.90	-10.4%	18.2%	-0.28	-0.52
21	608	617	29	3.7%	1.01	1.4%	4.7%	0.10	0.07
22	608	81	206	85.6%	0.13	-86.6%	33.9%	-3.34	-4.33
23	608	451	42	23.1%	0.74	-25.8%	6.9%	-0.71	-1.29
24	608	423	53	11.9%	0.70	-30.5%	8.8%	-1.48	-1.52
25	608	503	29	7.4%	0.83	-17.2%	4.7%	-1.00	-0.86
26	608	611	25	5.3%	1.01	0.5%	4.1%	0.03	0.03
27	608	>365.7	-	-	-	-	-	-	-
28	608	653	23	16.0%	1.07	7.4%	3.8%	0.20	0.37
29	608	674	69	3.5%	1.11	10.9%	11.4%	0.75	0.54

Lab Code	E _R	⟨E⟩	S _E	SL%	REF	Trueness%	Precision%	En	z- score
30	608	551	57	10.9%	0.91	-9.3%	9.4%	-0.40	-0.47
31	608	242	538	75.1%	0.40	-60.2%	88.6%	-0.99	-3.01
32	608	558	55	20.3%	0.92	-8.2%	9.0%	-0.21	-0.41
33	608	843	51	15.1%	1.39	38.6%	8.3%	0.88	1.93
34	608	675	40	15.6%	1.11	11.0%	6.6%	0.30	0.55
35	608	125	62	23.3%	0.20	-79.5%	10.1%	-5.14	-3.98
36	608	552	16	6.2%	0.91	-9.2%	2.7%	-0.55	-0.46
37	608	507	68	5.1%	0.83	-16.6%	11.1%	-1.11	-0.83
38	608	702	166	13.5%	1.15	15.4%	27.3%	0.46	0.77
39	608	584	26	6.8%	0.96	-4.0%	4.2%	-0.22	-0.20
40	608	619	40	12.0%	1.02	1.7%	6.5%	0.06	0.09
41	608	371	17	1.5%	0.61	-39.0%	2.8%	-3.17	-1.95
42	608	554	65	9.7%	0.91	-8.9%	10.7%	-0.42	-0.45
43	608	685	55	4.4%	1.13	12.7%	9.1%	0.81	0.64
44	608	636	467	24.5%	1.05	4.6%	76.8%	0.09	0.23
45	608	576	27	12.7%	0.95	-5.2%	4.4%	-0.19	-0.26
46	608	Data not received							
47	608	Data not received							
48	608	533	76	7.1%	0.88	-12.3%	12.5%	-0.70	-0.61
49	608	522	27	29.3%	0.86	-14.2%	4.5%	-0.27	-0.71
50	608	554	31	10.3%	0.91	-8.9%	5.2%	-0.40	-0.45

Table 5.3 Results - high exposure

Lab Code	E _R	⟨E⟩	S _E	SL%	REF	Trueness%	Precision%	En	z- score
1	8714	8377	197	6.1%	0.96	-3.9%	2.3%	-0.26	-0.19
2	8714	7596	101	1.4%	0.87	-12.8%	1.2%	-1.37	-0.64
3	8714	7963	134	5.0%	0.91	-8.6%	1.5%	-0.67	-0.43
4	8714	9921	1729	7.7%	1.14	13.8%	19.8%	0.70	0.69
5	8714	7002	184	7.1%	0.80	-19.6%	2.1%	-1.35	-0.98
6	8585	8161	372	5.3%	0.95	-4.9%	4.3%	-0.35	-0.25
7	8635	7785	242	5.5%	0.90	-9.8%	2.8%	-0.71	-0.49
8	8635	8535	144	4.5%	0.99	-1.2%	1.7%	-0.09	-0.06
9	8635	7362	98	2.8%	0.85	-14.7%	1.1%	-1.37	-0.74
10	8635	> 5000	-	-	-	-	-	-	-
11	8635	5624	60	0.6%	0.65	-34.9%	0.7%	-3.60	-1.74
12	8476	8432	584	5.5%	0.99	-0.5%	6.7%	-0.04	-0.03
13	8476	8079	399	5.4%	0.95	-4.7%	4.6%	-0.33	-0.23
14	8476	7343	122	7.6%	0.87	-13.4%	1.4%	-0.82	-0.67
15	8476	7337	174	7.8%	0.87	-13.4%	2.0%	-0.82	-0.67
16	8476	7623	273	2.5%	0.90	-10.1%	3.1%	-0.96	-0.50
17	8476	6317	1242	9.8%	0.75	-25.5%	14.3%	-1.46	-1.27
18	8476	5419	1442	15.4%	0.64	-36.1%	16.6%	-1.65	-1.80
19	8046	7625	172	1.8%	0.95	-5.2%	2.0%	-0.54	-0.26
20	8046	7832	1017	12.7%	0.97	-2.7%	11.7%	-0.10	-0.13
21	7648	9186	237	3.2%	1.20	20.1%	2.7%	1.62	1.01
22	7648	119	255	71.8%	0.02	-98.4%	2.9%	-9.84	-4.92
23	7648	4567	300	14.8%	0.60	-40.3%	3.4%	-1.99	-2.01
24	7648	7200	312	10.7%	0.94	-5.9%	3.6%	-0.26	-0.29
25	7648	6693	149	4.5%	0.88	-12.5%	1.7%	-1.00	-0.62
26	7648	7022	241	5.8%	0.92	-8.2%	2.8%	-0.57	-0.41

Lab Code	E _R	⟨E⟩	S _E	SL%	REF	Trueness%	Precision%	En	z- score
27	7648	> 4106	-	-	-	-	-		-
28	7158	7230	164	6.1%	1.01	1.0%	1.9%	0.06	0.05
29	7158	5490	42	0.4%	0.77	-23.3%	0.5%	-2.36	-1.17
30	7158	6997	355	10.4%	0.98	-2.3%	-4.1%	-0.10	-0.11
31	7158	8596	2724	16.2%	1.20	20.1%	31.3%	0.50	1.00
32	7357	5630	413	20.1%	0.77	-23.5%	4.7%	-0.72	-1.17
33	7158	10266	502	11.4%	1.43	43.4%	5.8%	1.27	2.17
34	6535	8259	294	10.6%	1.26	26.4%	3.4%	0.94	1.32
35	6535	1351	298	12.4%	0.21	-79.3%	3.4%	-7.65	-3.97
36	6535	6264	137	9.0%	0.96	-4.1%	1.6%	-0.21	-0.21
37	6535	5602	422	2.9%	0.86	-14.3%	4.8%	-1.39	-0.71
38	6535	6347	345	5.7%	0.97	-2.9%	4.0%	-0.20	-0.14
39	6535	4939	162	7.4%	0.76	-24.4%	1.9%	-1.70	-1.22
40	6535	5541	251	15.1%	0.85	-15.2%	2.9%	-0.56	-0.76
41	6535	3291	230	2.3%	0.50	-49.6%	2.6%	-5.32	-2.48
42	6535	6207	228	8.2%	0.95	-5.0%	2.6%	-0.28	-0.25
43	6535	5525	88	3.4%	0.85	-15.4%	1.0%	-1.44	-0.77
44	6535	5199	243	1.6%	0.80	-20.4%	2.8%	-2.18	-1.02
45	6535	5319	167	18.0%	0.81	-18.6%	1.9%	-0.61	-0.93
46	5900	Data not received							
47	5900	Data not received							
48	5900	6545	442	5.6%	1.11	10.9%	5.1%	0.71	0.55
49	5900	7265	139	14.5%	1.23	23.1%	1.6%	0.63	1.16
50	6155	5640	341	9.4%	0.92	-8.4%	3.9%	-0.43	-0.42

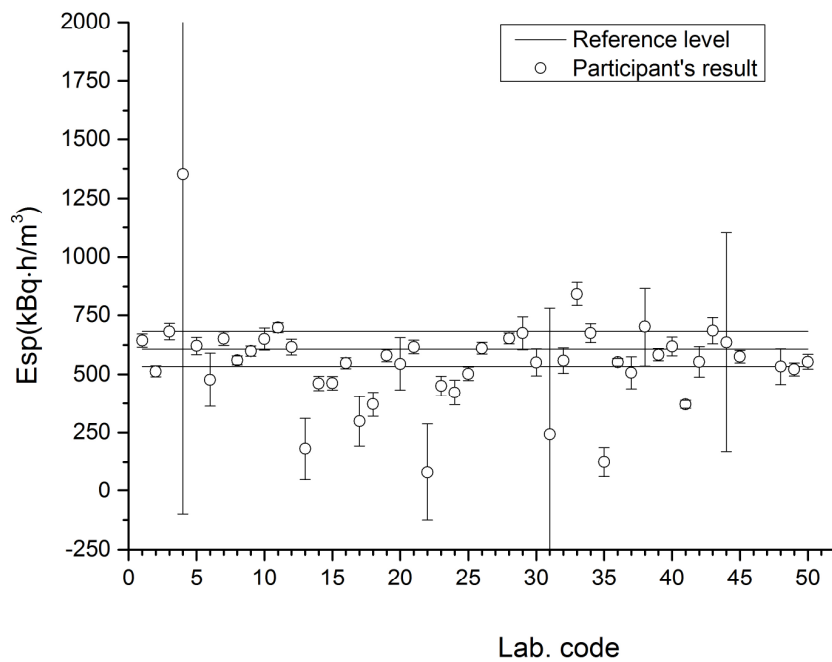


Figure 5.1. *Low exposure:* results of the participants $\langle E \rangle$ with their standard deviations compared to the reference level (solid line) and its uncertainty ($k=1$, grey lines).

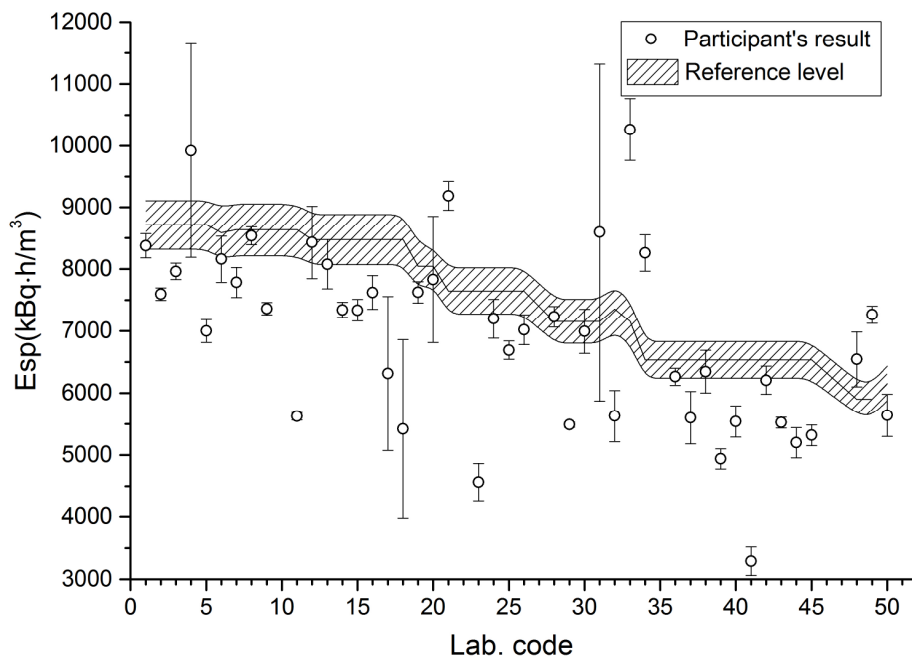


Figure 5.2. *High exposure:* results of the participants $\langle E \rangle$ with their standard deviations compared to the different reference levels (solid line) and their uncertainties ($k=1$, grey lines).

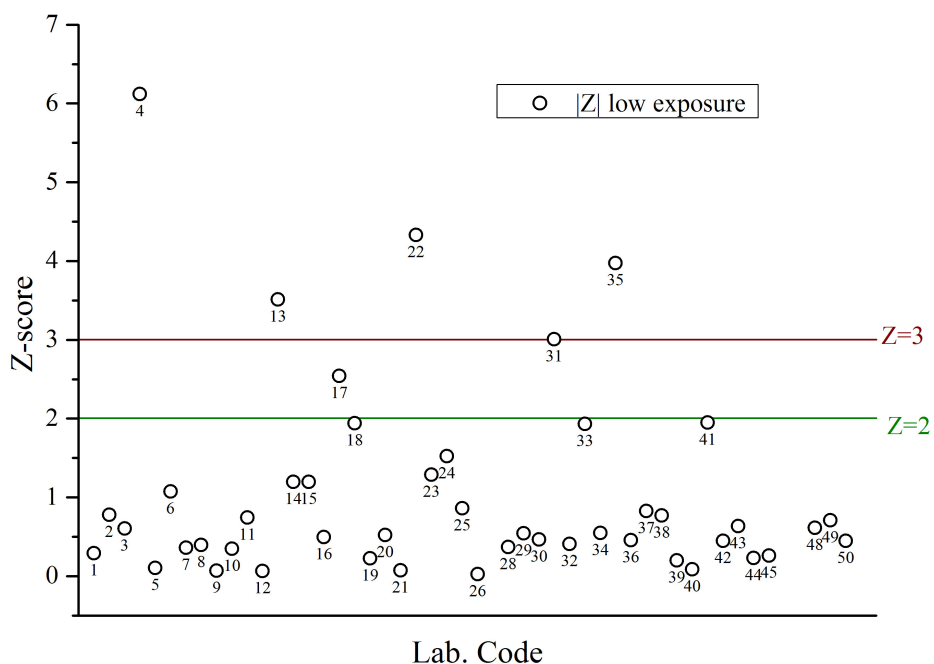


Figure 5.3. *Low exposure* - Absolute values of the z-score. Values above 2 and 3 are highlighted: following the ISO, are considered acceptable values < 2. Values in the range 2-3 give a warning. Values above 3 are considered unacceptable.

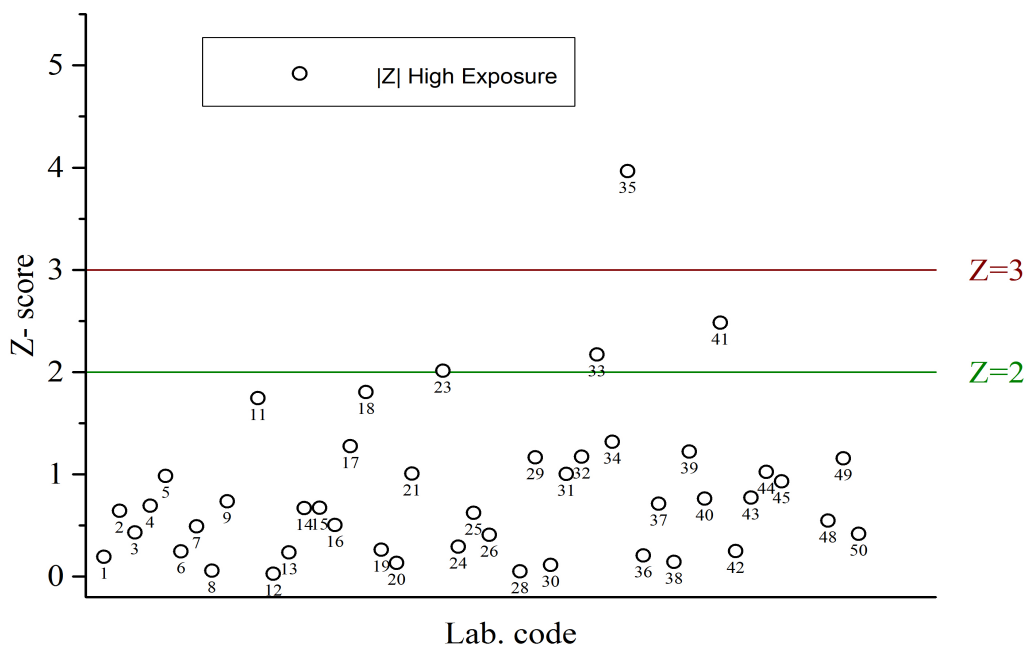


Figure 5.4. *High exposure* - Absolute values of the z-score. Values above 2 and 3 are highlighted: following the ISO, are considered acceptable values < 2. Values in the range 2-3 give a warning. Values above 3 are considered unacceptable.

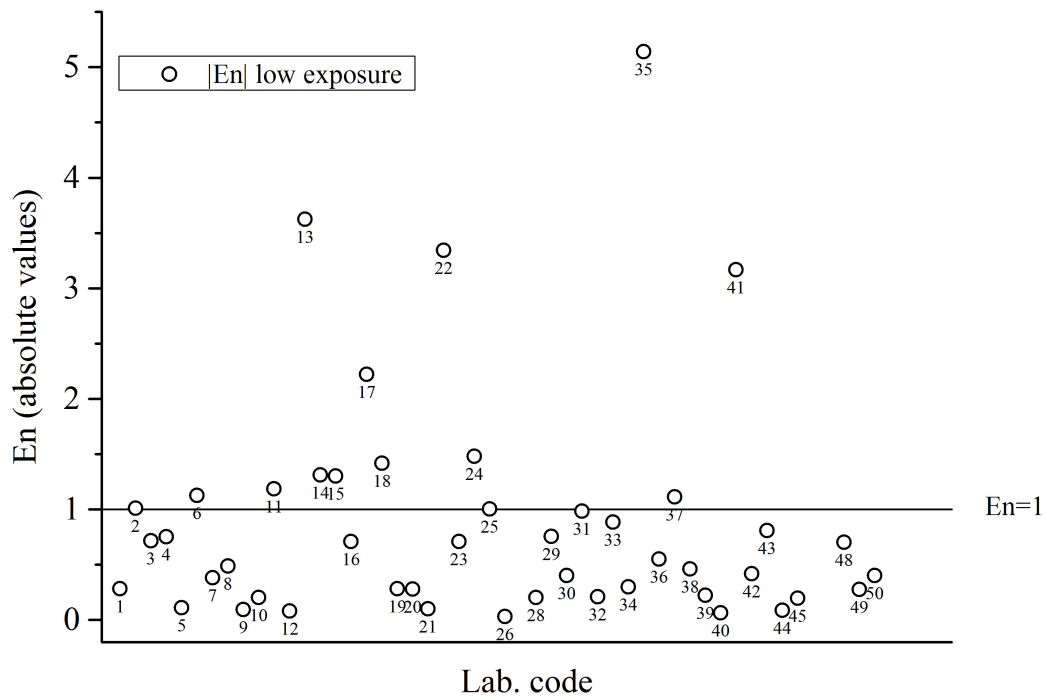


Figure 5.5. Absolute value of E_n for the low exposure.

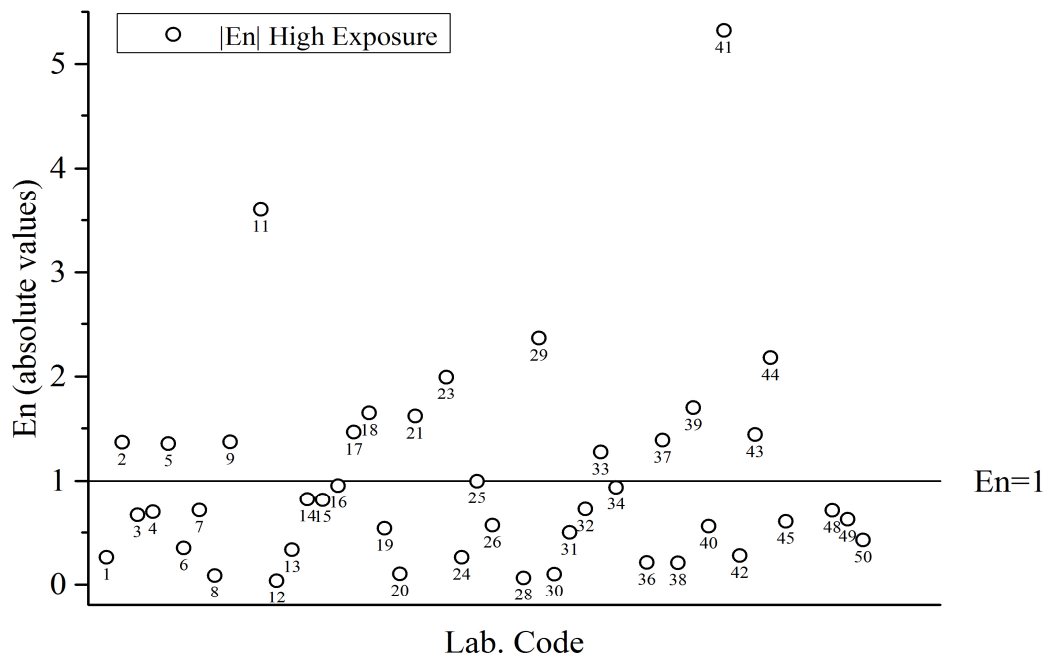


Figure 5.6. Absolute value of E_n for the high exposure.

For the normalized error E_n the acceptable values are those < 1 (absolute value). In the Figures 5.5 and 5.6 the E_n values for the low and high exposures respectively, are shown.

It can be observed that the criterion $E_n < 1$ is by far more strict than the one based on the z-score value. In fact, in this case, the laboratories that gave unacceptable results are much more: the 28% for the low exposure and the 30% for the high exposure.

To evaluate the performance of the labs taking into account at the same time both the exposures (low and high), it is possible to use the Youden plot, as shown in Figure 5.7. With this technique, the performance of the laboratory is measured by the distance between a point whose coordinate are given by the experimental values of the two exposures and the centre of a circle. In this plot, the distance from the bisector quantifies the relevance of the systematic errors.

It can be noticed that in this plot about 80% of the participants lies in the area 1, limited by a circle representing the 95% confidence interval: these data can therefore be considered acceptable. The 7 laboratories (15.5%) whose values are outside the circle but close to the bisector (areas 2 and 3 of the plot), show a good reproducibility but poor accuracy. Only 2 laboratories (4.5%), in the areas 4 and 5, gave totally unacceptable data, having at the same time poor accuracy and poor reproducibility.

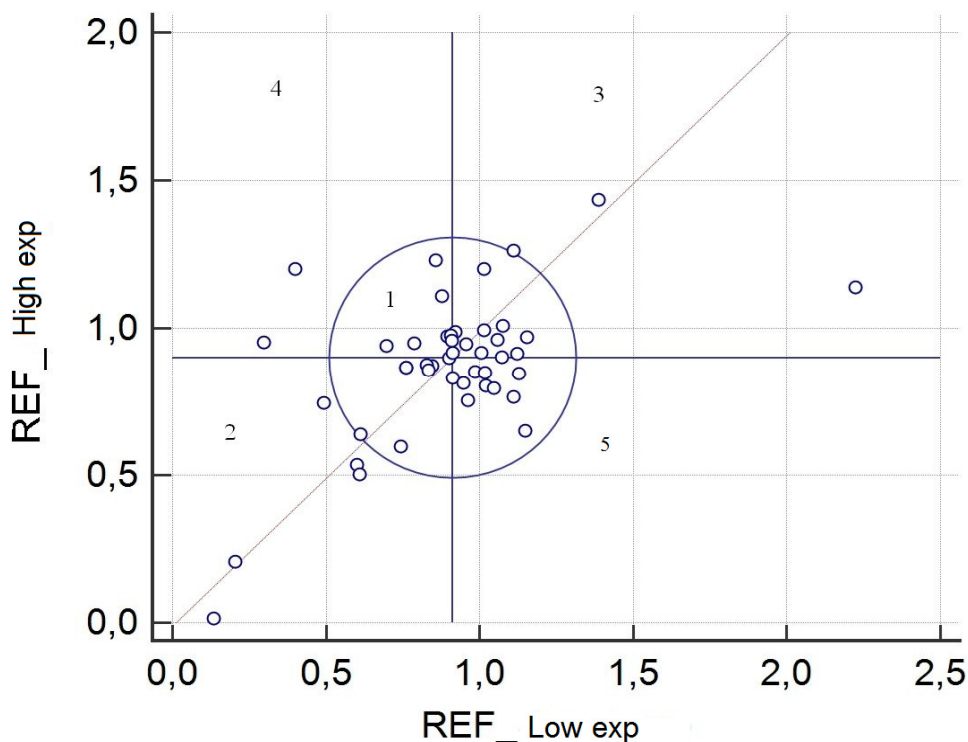


Figure 5.7. Youden Plot: 80% of the labs are within the circle representing the 95% confidence interval.

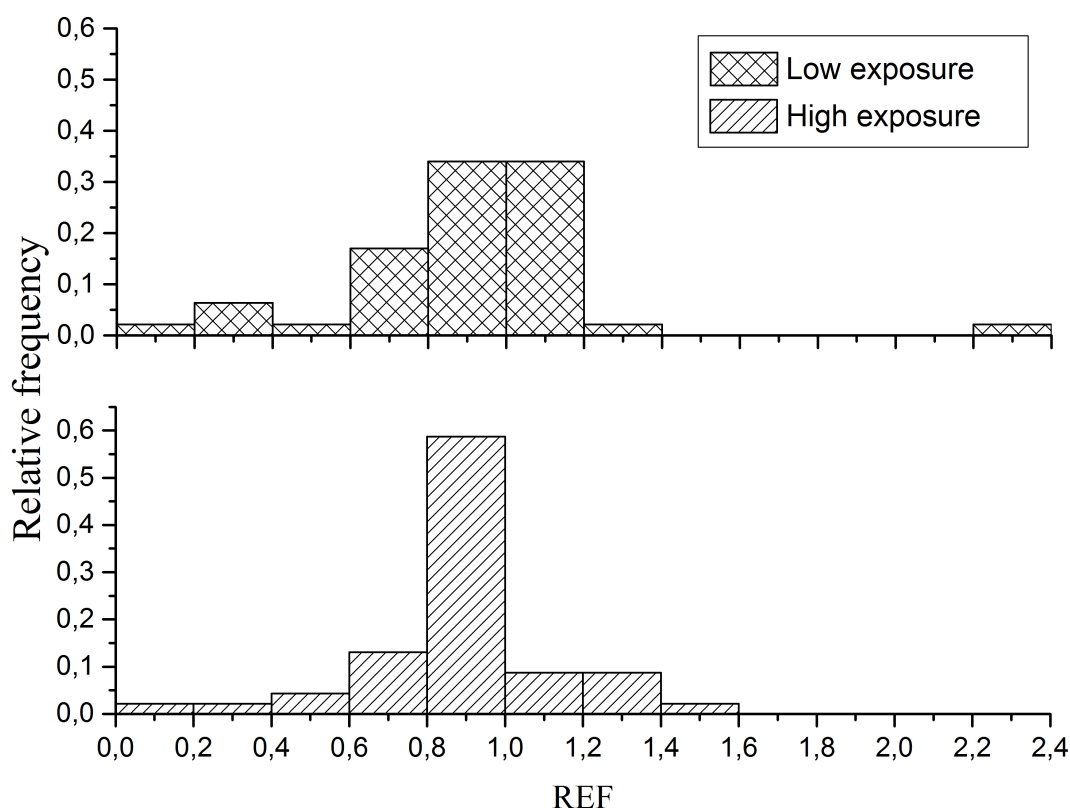


Figure 5.8. Distribution of the exposure values normalized to the reference value; above the data of the low exposure, below the data of the high exposure.

In Figure 5.8 the normalized distributions of the data are presented. The histograms look quite asymmetric, with a substantial predominance of values < 1, more evident for the high exposure.

The observed global trend of a substantial underestimation of the real radon concentration can be pointed out even more clearly by using the Mendel's graphics, shown in the following Figure 5.9 and 5.10. The Mandel index h is a parameter used for the evaluation of the consistency between laboratories. This index is defined for the generic j -th laboratory by the following formula:

$$h_j = \frac{\langle E \rangle_j - E_R}{S_{Ej}}$$

where S_{Ej} is the standard deviation for normally distributed data.

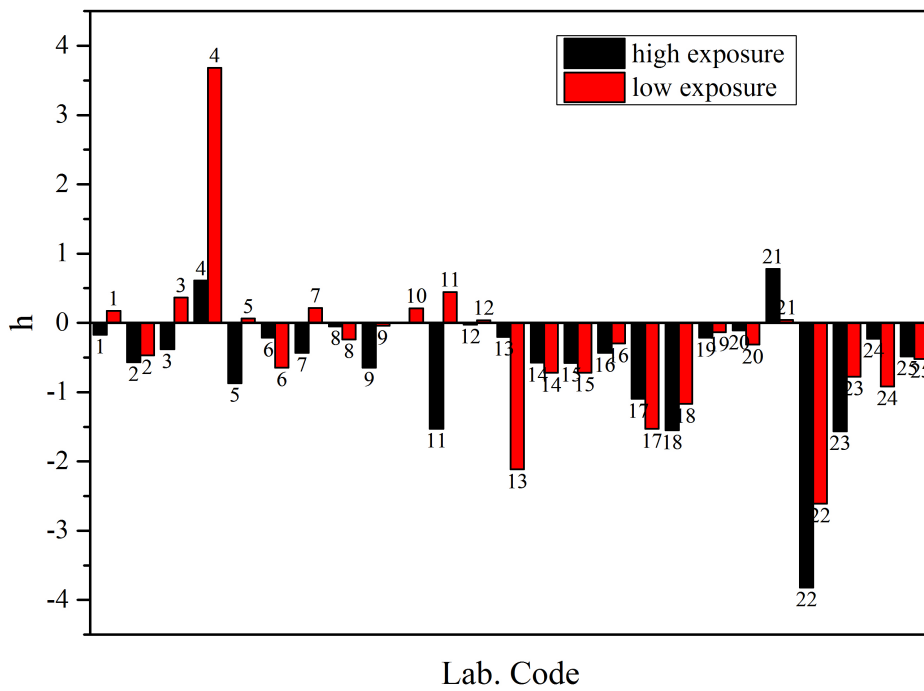


Figure 5.9. Mandel plot for the normalized the data sets ID 1-25.

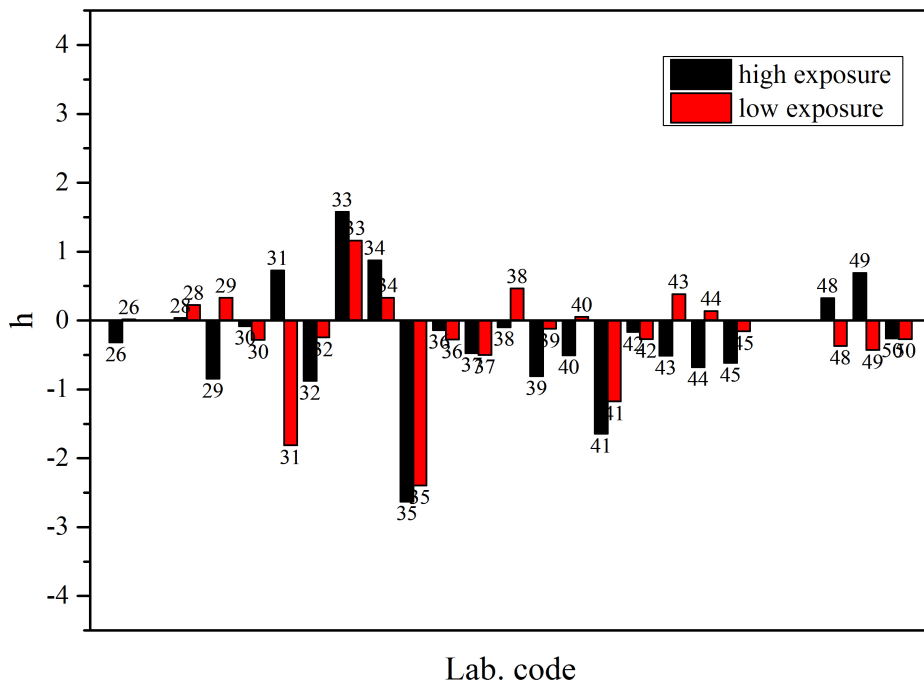


Figure 5.10. Mandel plot for the normalized data sets ID 26-50.

5.2 Statistical analysis

In the following data analysis we have considered as input data the “net exposure values”, i.e., the experimental values minus the transit contribution. For each data set a box plot was generated.

The box plot in descriptive statistics is used as a tool for representing graphically the distribution of the data by means of the quartiles. The box contains the 50% of the data, being defined as the interquartile range $IQR=Q3-Q1$ ($Q3 = 75^{\circ}$ percentile; $Q1 = 25^{\circ}$ percentile) and it is internally divided by the median. The two segments outside the box, called “whiskers”, can be defined in many different ways: in our case, the lower whisker is defined as $Q1-1.5 \cdot IQR$ while the upper whisker is $Q3+1.5 \cdot IQR$.

So, the box plot allows to graphically visualize the distribution of the data as well as the occurrence of some outliers, eventually displayed outside the whiskers.

In Figure 5.11 and 5.12 the box plots for each data set and for both the exposures, are shown.

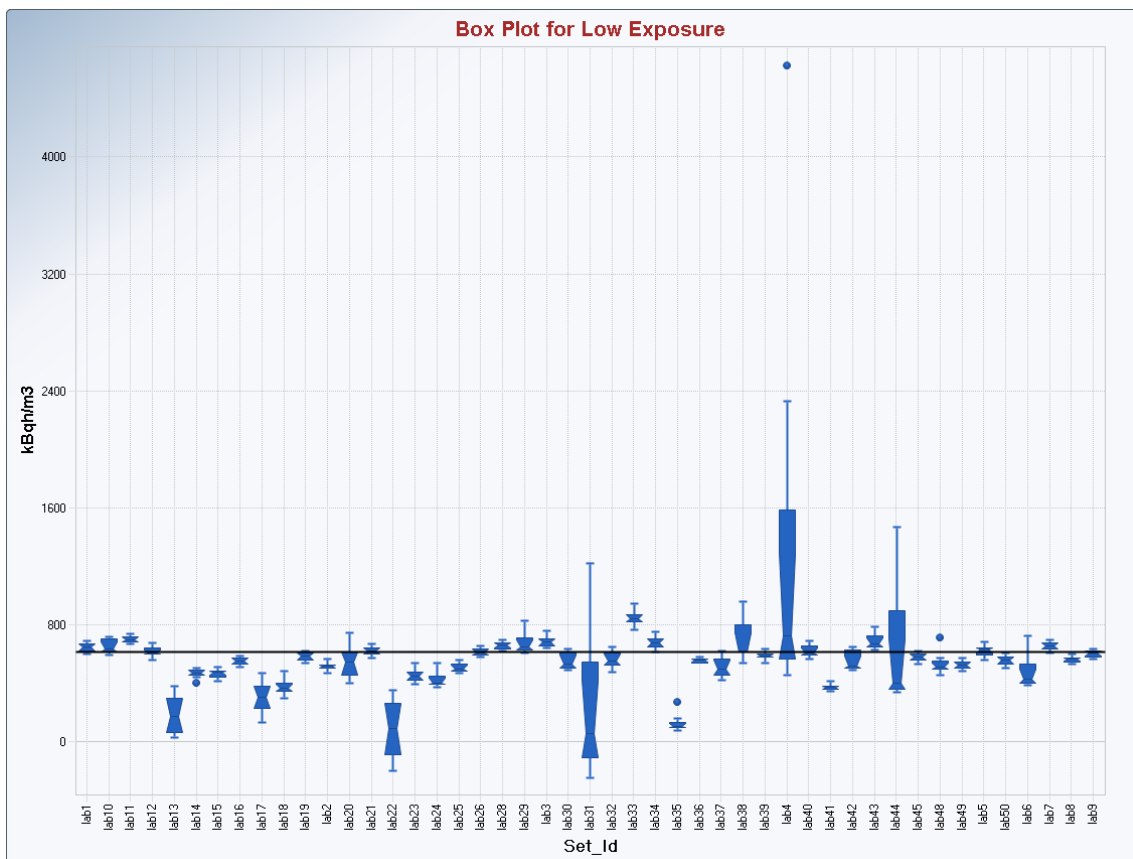


Figure 5.11. Box plots for the low exposure: the points outside the whiskers are the possible outliers.

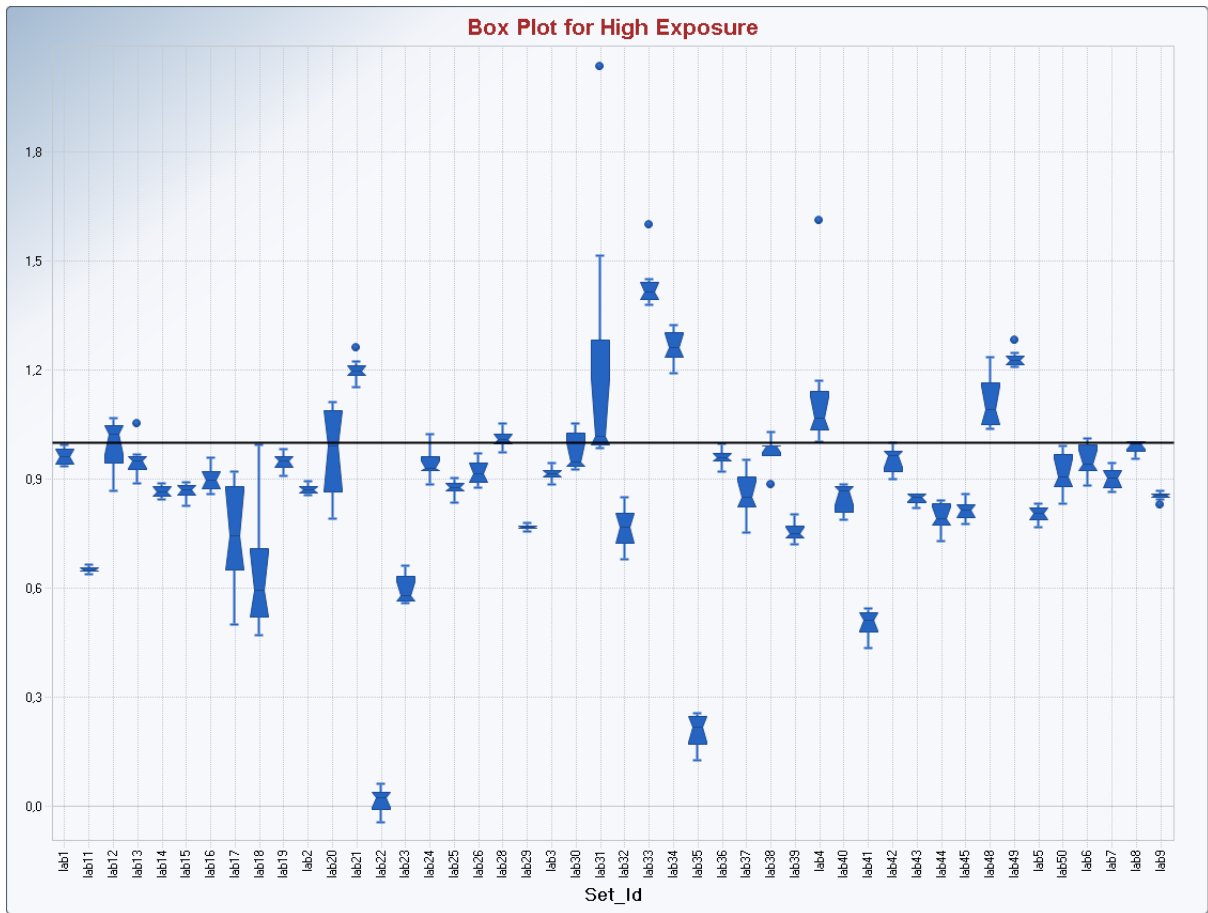


Figure 5.12. Box plots for the high exposure: the points outside the whiskers are the possible outliers. The reference value (solid line) is normalized to 1.

The box plots show, in many cases, some possible outliers. In order to identify them, the Dixon test, suitable for small data sets, was performed on all the available data sets. The Dixon test is applied on an ordered growing series of data. In particular, for a series of n data x_n , with $x_n > x_{n-1}$, the quantity C_n is calculated as follows:

$$C_n = \frac{|x_n - x_{n-1}|}{R}$$

where R is the range spanned by the x_n data set. A value x_n will be considered as an outlier at a specified confidence level α if $C_n > C_v$, where C_v is a tabulated critical level at the α confidence level.

The Dixon test can be used for the outliers evaluation if the sample size is ≤ 25 and if the data can be considered normally distributed. If the latter condition is not fulfilled, the Tukey test should be applied. Following this approach, those data outside two threshold values are defined as outliers; in particular:

- < $Q1 - 1.5 \cdot IQR$
- > $Q3 + 1.5 \cdot IQR$

The list of the outliers identified using the Dixon test (at a significance level $\alpha=5\%$) for both the low and the high exposure are reported in the following Table 5.4.

Table 5.4 List of the outliers identified using the Dixon test

Low Exposure	High Exposure
Laboratory ID4: 4626 e 2321 kBqh/m ³	
Laboratory ID14: 399 kBqh/m ³	Laboratory ID4: 14051 kBqh/m ³
Laboratory ID31: 1214 kBqh/m ³	Laboratory ID49: 7569 kBqh/m ³
Laboratory ID35: 150 e 268 kBqh/m ³	Laboratory ID13: 8922 kBqh/m ³
Laboratory ID44: 1315 e 1457 kBqh/m ³	Laboratory ID33: 11446 kBqh/m ³
Laboratory ID48: 705 kBqh/m ³	

After the elimination of these values, we checked all the distributions for normality: all the sets resulted normal except those of the lab. ID31, for both exposures. We therefore applied to these data the Tukey test and finally we found the following outliers:

- 954 kBq·h·m⁻³ for the low exposure;
- 10818 e 14568 kBq·h·m⁻³ for the high exposure.

In Figures 5.13 and 5.14 the box plot after the exclusions of all the outliers are reported. It can be easily seen that, in many cases, the outliers elimination improves not only the symmetry of the distributions but also the estimations of the mean that become very close to the reference levels. This happens in particular for the lab. ID4 (low exposure) and for the lab 31 (high exposure). In fact, for the lab. ID4, the mean changes from 1352 kBqhm⁻³ to 645 kBqhm⁻³ while the median changes from 720 kBqhm⁻³ to 649 kBqhm⁻³. Similarly, for the lab. ID31, the mean value 8596 kBqhm⁻³ reduces to 7282 kBqhm⁻³ and the median 7231 kBqhm⁻³ becomes 7175 kBqhm⁻³.

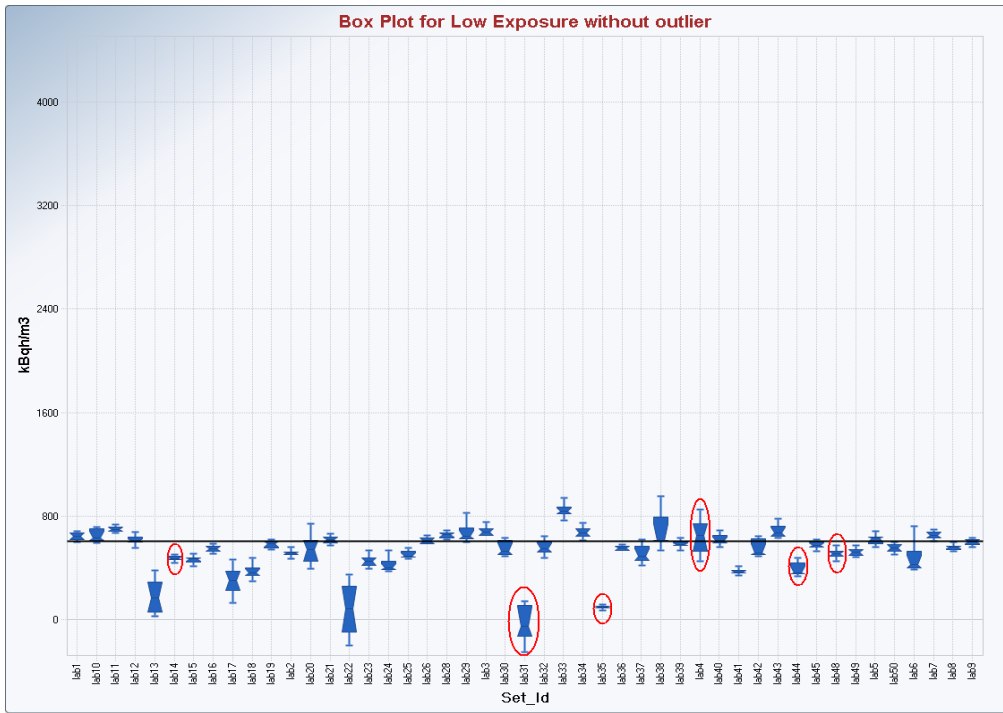


Figure 5.13. Low exposure box plots after the outliers elimination: in red the data set modified (see Figure 5.11 for comparison).

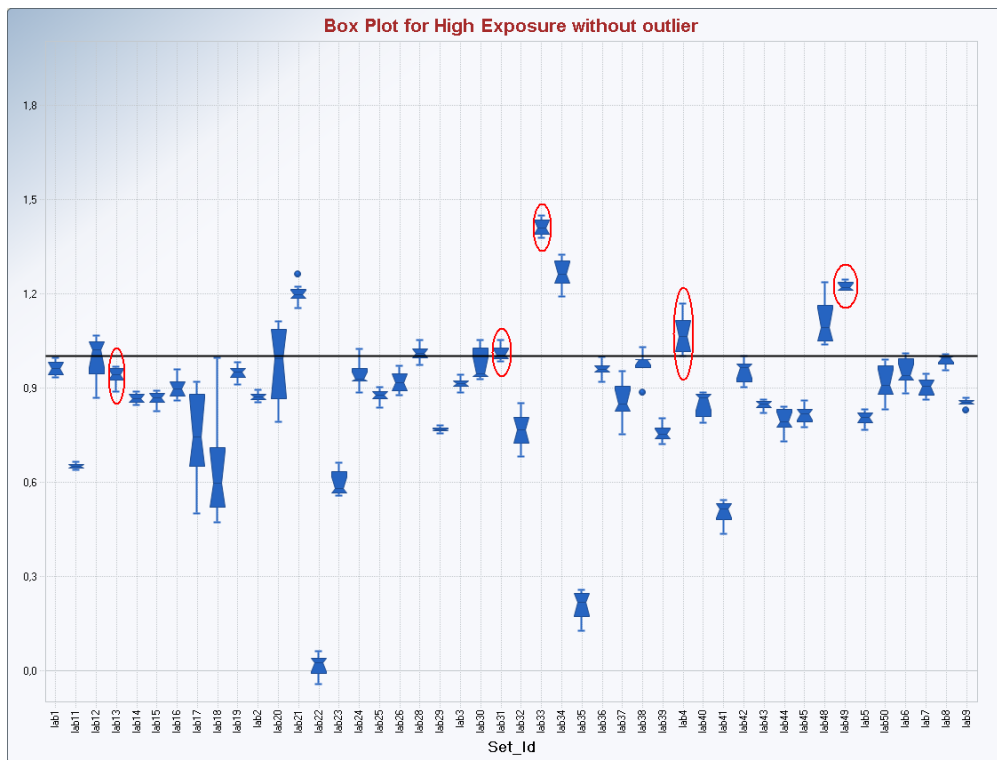


Figure 5.14. Low exposure box plots after the outliers elimination: in red the data set modified (see Figure 5.11 for comparison).

6. Conclusions

It is not an easy task to reach a comprehensive judgment of the results presented and briefly discussed in this report. Anyway, the principal aim of this publication was simply to give all the participants to this exercise some food for thought, comparing their own results to those obtained by the others. It is up to everybody to take from this experience the most important lesson for themselves.

It was thus decided, as a precise and conscious choice of the organizers, to not establish a unique criterion for the evaluation of the performances. Many reasons suggested this approach: the most important one is the fact that the great difficulty and complexity typical of the “in-field intercomparison” would have made questionable any definition of criteria for the listing of a rank.

We preferred instead to simply calculate and discuss a number of different indicators such as trueness, precision, normalized error E_n , z-score, Youden plot, without giving any ranking criteria. Our comments and considerations on the results obtained by the labs generally followed the ISO suggestions. We made only one arbitrary choice, assuming for the parameter σ_R that appears in the z-score definition, a value corresponding to the 20% of the reference value.

References

- [1] J. L. Gutierrez-Villanueva et al., International intercomparison exercise on natural radiation measurements under field conditions, PUBliCan Edicione Universidad de Cantabria (2012).
- [2] R Core Team (2014). R. A language and environment for statistical computing. R Foundation for statistical Computing, Vienna, Austria. URL <http://www.R-project.org/>.
- [3] F. Cardellini et al., Interconfronto radon in aria per sistemi di misura passivi nella grotta di Marie Curie a Lurisia, Convegno Nazionale di Radioprotezione, Aosta (15-17 ottobre 2014), in Italian, ISBN 978-88-886484-0-8; <http://airp-asso.it>.
- [4] ISO/IEC 17043:2010. Conformity assessment - General requirements for proficiency testing.
- [5] ISO 13528: 2005. Statistical methods for use in proficiency testing by interlaboratory comparisons.
- [6] Z. Daraktchieva et al., Result of the 2013 PHE Intercomparison of Passive Radon Detectors.
- [7] E. Foerster et al., Instruments to Measure Radon Activity concentration or Exposure to Radon – Interlaboratory Comparison 2012.
- [8] ProUCI 5.0, www.epa.gov.